UNIVERSIDADE DE BRASÍLIA
FACULDADE DE AGRONOMIA E MEDICINA VETERINÁRIA

ESTUDO DE CRANIOMETRIA TOMOGRÁFICA E DESCRIÇÃO DO TRAJETO NASOLACRIMAL EM FELINOS DOMÉSTICOS (*Felis catus*)

ROGÉRIO LOPES DA FONSECA

TESE DE DOUTORADO EM CIENCIAS ANIMAIS

BRASÍLIA/DF
MARÇO DE 2020

UNIVERSIDADE DE BRASÍLIA
FACULDADE DE AGRONOMIA E MEDICINA VETERINÁRIA

ESTUDO DE CRANIOMETRIA TOMOGRÁFICA E DESCRIÇÃO DO TRAJETO NASOLACRIMAL EM FELINOS DOMÉSTICOS (*Felis catus*)

ROGÉRIO LOPES DA FONSECA

ORIENTADORA: PROFA. DRA. PAULA DINIZ GALERA

TESE DE DOUTORADO EM CIENCIAS ANIMAIS

PUBLICAÇÃO: 223D/2020

BRASÍLIA/DF
MARÇO DE 2020

REFERÊNCIA BIBLIOGRÁFICA E CATALOGAÇÃO

FICHA CATALOGRÁFICA

FONSECA, Rogério Lopes. **ESTUDO DE CRANIOMETRIA TOMOGRÁFICA E DESCRIÇÃO DO TRAJETO NASOLACRIMAL EM FELINOS DOMÉSTICOS (*Felis catus*)**. Brasília: Faculdade de Agronomia e Medicina Veterinária da Universidade de Brasília, 2020. 80p. Tese (Doutorado em Ciências Animais) – Faculdade de Agronomia e Medicina Veterinária da Universidade de Brasília, 2020.

1. Braquicefálico. 2. Craniometria. 3. Ducto nasolacrimal. 4. Felinos. 5. Tomografia. I. Galera, P.D. PhD. II. Título

UNIVERSIDADE DE BRASÍLIA
FACULDADE DE AGRONOMIA E MEDICINA VETERINÁRIA

ESTUDO DE CRANIOMETRIA TOMOGRÁFICA E DESCRIÇÃO DO TRAJETO NASOLACRIMAL EM FELINOS DOMÉSTICOS (*Felis catus*)

ROGÉRIO LOPES DA FONSECA

TESE DE DOUTORADO SUBMETIDA AO PROGRAMA DE PÓS-GRADUAÇÃO EM CIÊNCIAS ANIMAIS, COMO PARTE DOS REQUISITOS NECESSÁRIOS À OBTENÇÃO DO GRAU DE DOUTOR EM CIÊNCIAS ANIMAIS.

APROVADA POR:

_____

Profa. PAULA DINIZ GALERA, DOUTORA (UNIVERSIDADE DE BRASÍLIA - UnB) (ORIENTADORA)

_____

Prof. ADALFREDO ROCHA LOBO-JUNIOR, DOUTOR (UNIVERSIDADE FEDERAL DOS VALES DO JEQUITINHONHA E MUCURI) (EXAMINADOR EXTERNO)

_____

Prof. MARCELO ISMAR SILVA SANTANA, DOUTOR (UNIVERSIDADE DE BRASÍLIA - UnB) (EXAMINADOR EXTERNO)

_____

Profa. NAIDA CRISTINA BORGES, DOUTORA (UNIVERSIDADE FEDERAL DE GOIÁS - UFG) (EXAMINADORA EXTERNA)

BRASÍLIA/DF, 06 DE MARÇO DE 2020.

DEDICATÓRIA

Dedico primeiramente a Deus, por me capacitar e ser meu porto seguro, abrigo na tempestade e refúgio na angústia. À minha maravilhosa esposa Iracylka, que sempre foi sábia, compreensiva, incentivadora e cooperadora. Aos meus filhos, Eduardo, Milena e Fernanda que representam as mais preciosas dádivas que um pai pode receber.

AGRADECIMENTOS

A Deus, que ainda no ventre de minha mãe, me escolheu e tem me capacitado a chegar a mais este momento especial em minha vida, sempre na Sua dependência;

Ao meu pai Iraci e à minha mãe Maria, fieis e resilientes, que mesmo tendo origens humildes projetaram e lançaram palavras de bênçãos sobre os filhos;

À minha linda esposa Iracylka, pelo companheirismo e amor, estando sempre ao meu lado em todos os momentos, essa vitória é nossa;

Aos meus filhos, Eduardo, Milena e Fernanda, seres humanos esplêndidos, fontes de motivação, com quem aprendo diariamente;

Aos meus irmãos, Edmar e Ademir, pelo exemplo, eterno apoio e incentivo;

À Universidade de Brasília pela oportunidade, em especial ao Programa de Pós-Graduação em Ciências Animais; A CAPES pelo suporte e apoio indispensáveis a execução deste manuscrito;

À minha orientadora Paula Diniz Galera, pela oportunidade, confiança, incentivo, compromisso e inspiração;

Ao meu Co-orientador, Marcelo Ismar Silva Santana, pela sua grande colaboração e apoio durante todo o período de mestrado e doutorado;

Ao Professor Adalfredo Rocha Lobo-Junior, pelo auxílio, prontidão e assertividade nos apontamentos, colaborando para melhoria do trabalho;

Aos colegas de pós-graduação, agradeço pelas trocas de conhecimento ao longo do curso;

A todos os professores, funcionários da instituição e convidados que participaram e acrescentaram algo ao curso;

A todos os amigos e conhecidos, que de alguma forma colaboraram ou fizeram parte dessa história e por ventura tenha esquecido, fica aqui meu sincero muito obrigado!

ÍNDICE

RESUMO

ESTUDO DE CRANIOMETRIA TOMOGRÁFICA E DESCRIÇÃO DO TRAJETO NASOLACRIMAL EM FELINOS DOMÉSTICOS (*Felis catus*)

Rogério Lopes da Fonseca[1], Paula Diniz Galera[1]

[1]Laboratório de Oftalmologia Comparativa, Faculdade de Agronomia e Veterinária, Universidade de Brasília, Brasília, DF, Brazil (UnB)
rogerio.vet1000@gmail.com

Objetivou-se: 1) investigar a morfometria craniana de felinos domésticos de focinho curto e não curto e 2) descrever o trajeto do ducto nasolacrimal de gatos Persas. Foram mensurados o índice craniano (IC) e o ângulo crânio-facial (CFA) de trinta (30) animais, que foram divididos em dois grupos: gatos pelo curto brasileiro (BSH) e Persas, de acordo com o fenótipo craniano. Para descrição do ducto nasolacrimal, foi utilizado o grupo dos 10 (dez) gatos de focinho curto (Persas). Foi realizada a dacriocistografia computadorizada (DCG-CT) em todo o grupo, e 2 (dois) animais foram submetidos à dissecação craniana, com moldes do ducto nasolacrimal previamente fixados com látex. Foram mensurados o comprimento e o diâmetro do ducto nasolacrimal, dos canalículos lacrimais, e a menor distância entre ducto nasolacrimal e a raiz do dente canino superior, além da avaliação dos pontos de estenose e tortuosidade do ducto. As análises estatísticas incluíram análise descritiva, de variância, de correlação e de regressão, para comparar e melhor compreender possíveis relações entre as variáveis estudadas. Os valores médios de IC e CFA para BSH e gatos Persas foram de 61,7 e 78,7% e 12,0 e 9°, respectivamente. Apenas dois tipos cranianos foram identificados, diferentemente do que ocorre em cães, com base na associação desses dois parâmetros craniométricos: braquicefálicos, em gatos Persas; e não braquicefálicos, em gatos BSH. Esses valores de referência para gatos com focinho curto (Persas) e longo (BSH) foram determinados de maneira inédita e poderiam ser utilizados para classificação
fenotípica dos crânios de gatos. Em todos os gatos de focinho curto o ducto nasolacrimal apresentou trajeto tortuoso, estenoses e dilatações. O comprimento do ducto nasolacrimal

variou de 1,3 a 1,5 cm, com diâmetro entre 1,5 mm e 2,34 mm. O comprimento médio dos canalículos foi de 3,1 mm e o diâmetro médio, de 0,4 mm. Não foram encontradas aberturas acessórias do ducto nasolacrimal, contrariamente aos relatos anteriores.

Palavras chave: brachycephaly, craniofacial angle, cranial index, felines, nasolacrimal duct, Persians.

ABSTRACT

COMPUTED TOMOGRAPHIC CRANIOMETRY AND DESCRIPTION OF NASOLACRIMAL DUCT TRAJECTORY IN DOMESTIC CATS

Rogério Lopes da Fonseca,[1] Paula Diniz Galera[1]

Comparative Ophthalmology Laboratory, School of Agricultural Sciences and Veterinary Medicine, University of Brasília, Brasília, DF, Brazil.
rogerio.vet1000@gmail.com

This study set out to investigate skull morphometry in short-nosed and long-nosed domestic cats and to describe the nasolacrimal duct trajectory in short-nosed cats. The cephalic index (CI) and the craniofacial angle (CFA) of thirty (30) cats were measured using computed tomography. Cats were allocated to one of two groups according to skull phenotype, as follows: Brazilian short-haired (BSH) and Persian cats. Ten (10) short-nosed (Persian) cats were submitted to computed tomographic dacryocystography (CT-DCG); of these, two (2) were also submitted to skull dissection following latex injection into the nasolacrimal duct. Nasolacrimal duct and lacrimal canaliculi length and width and the shorter distance between the nasolacrimal duct and the root of the upper canine tooth were measured. Nasolacrimal duct tortuosities and stenoses were also investigated. Statistical analyses (descriptive statistics, analysis of variance, correlation and regression analysis) were conducted to compare and investigate potential relationships between variables. Mean IC and CFA corresponded to 61.7 and 78.7% and 12.0 and 9° (BSH and Persian cats respectively). In contrast with dogs, combined craniometric parameters in this study revealed only two skull types: brachycephalic and non-brachycephalic (Persian and BSH cats respectively). Craniometric reference ranges for short- and long-nosed cats (Persian and BSH cats respectively) had not been reported to date and may be used for phenotypic classification of the feline skull. Tomographic assessment revealed tortuous nasolacrimal duct trajectory (middle and rostral portions in particular) determined by shortened facial bones. Stenoses (width reduction equal to or greater than 75%) and dilations (width increase equal to or greater than 50%) were also detected, particularly in the rostral portion of the duct. Nasolacrimal duct length and width ranged from 1.3 to 1.5 cm and 1.5

and 2.34 mm respectively. Mean lacrimal canaliculi length and width corresponded to 3.1 mm and 0.4 mm respectively. The root of the canine tooth interfered with duct trajectory. The short distance (mean distance, 2.4 mm) between the root of the maxillary canine tooth and the nasolacrimal duct predisposes brachycephalic cats to extramural duct inflammation secondary to periodontal disease and tooth extractions. Different from dogs, cats in this study had dilated lacrimal sacs. This feature may be associated with high rates of epiphora and negative responses in the Jones lacrimal drainage assessment test in this species. In contrast with previous reports, no accessory nasolacrimal duct openings were found in this study.

Key-words: brachycephaly, craniofacial angle, cranial index, felines, nasolacrimal duct, Persians.

LISTA DE ABREVIAÇÕES E SIGLAS

BSH	Brazilian Shorthair Cats
CFA	Craniofacial Angle
cm	centimeter
CT	Computed Tomography
CV	Coefficient of Variation
DCG-CT	Computerized dacryocystography
HU	Hounsfield scale
CI	Cranial Index
IU	International Unit
kV	Kilovolt
mA	miliAmpere
mL	milliliter
mm	millimeter

LISTA DE TABELAS

CAPÍTULO 2

CAPÍTULO 3

LISTA DE FIGURAS

CAPÍTULO 2

CAPÍTULO 3

CAPÍTULO 1

INTRODUÇÃO E REVISÃO DE LITERATURA

1. INTRODUÇÃO

O gato doméstico (*Felis catus*, Linnaeus, 1758) é um carnívoro com distribuição mundial (Lipinski et al., 2008). Muitas das raças felinas tiveram um desenvolvimento "natural", ou seja, não associado a um processo de seleção artificial (Kurushima et al., 2012). Entretanto, nos últimos 150 anos, uma variedade de gatos com pedigree foi desenvolvida devido à seleção artificial imposta pela humanidade no processo de domesticação desta espécie. Aproximadamente 85% das raças existentes foram desenvolvidas nos últimos 80 anos, por meio de seleção fenotípica, associadas a um único gene. As populações de felinos domésticos de raça definida são mais variáveis do ponto de vista genético, assim a manifestação de fenótipos homozigóticos é 10% maior nessas populações, podendo trazer consigo anormalidades anatômico-funcionais (Parker et al., 2004; Lipinsk et al., 2008; Zhao et al., 2012; Gandolfi et al., 2013; Kim et al., 2015).

O crânio felino representava uma harmonia arquitetônica na relação entre forma e função, previamente às interferências de seleção artificial. O crânio facilitava a ingestão e a respiração, fornecendo proteção para o cérebro, abrigando os sistemas visual, auditivo e olfativo, além de contribuir para a comunicação, defesa e reprodução desses animais. A intervenção humana sobre a redução do formato craniano modificou amplamente a influência da seleção natural sobre a forma e função, atendendo propósitos humanos e deixando de lado o bem-estar animal (Bertolini et al. 2016).

O formato do crânio é o critério mais importante utilizado para se determinar o padrão racial em gatos, sendo a craniometria uma das principais ferramentas na avaliação das características raciais desta espécie. A apresentação fenotípica da cabeça do gato doméstico depende da forma óssea e está muito relacionado com as propriedades esqueléticas específicas da raça. Com base em determinados pontos craniométricos é possível estabelecer medidas

lineares e angulares. Estas medidas caracterizam as diferentes raças e permitem a classificação desses animais em grupos, de acordo com o tipo craniano (Regodón et al. 1993; Wehausen & Ramsey, 2000; Constantinescu, 2005).

Esta classificação, entretanto, é divergente em opiniões. Künzel et al. (2003) descreveram a craniometria em felinos domésticos classificando-os em crânios arredondados, cuneiformes ou triangulares, tendo como exemplos de extremos fenotípicos o gato Siamês e o Persa. Entretanto, Done et al. (1990) relatam apenas duas categorias: braquicefálico e dolicocefálico, evidenciando controvérsias sobre o assunto, que atribui a essa espécie uma nomenclatura baseada apenas em critérios fenotípicos (Künzel et al., 2003).

A braquicefalia é um termo usado para descrever uma malformação congênita que resulta em um crânio desproporcionalmente curto e largo (Pollinger et al., 2005). Trata-se de uma condrodisplasia associada aos ossos basioccipital e basefenoide levando ao fechamento precoce das cartilagens da base do crânio, o que resulta no encurtamento do eixo longitudinal do mesmo. Isso pode provocar síndromes patogênicas como anomalias respiratórias e mastigatórias, fissuras labial e palatina, associação a gliomas, doenças oftalmológicas como epífora, exoftalmia, lagoftalmia, triquíase e entrópio do canto medial, predisposição à ceratoconjuntivite seca (CCS), ceratite pigmentar, úlceras de córnea, trauma ocular, tortuosidade dos ductos lacrimais e outras alterações patológicas (Hayes et al. 1975; Aron & Crowe, 1985; Williams et al., 2012; Breit et al., 2003; Schlueter et al., 2009; Labelle et al., 2013).

Graus elevados de braquicefalia também estão associados a malformações da calota craniana e ossos faciais, bem como malformações dentárias. Recentemente, a base genética da braquicefalia em gatos Persas foi investigada apontando dois genes responsáveis: CNTN6 e CHL1 (Bertolini et al. 2016). Em alguns animais dessa raça, essas mudanças resultaram da seleção para produzir um fenótipo extremo, fazendo deles bons representantes do fenótipo braquicefálico. Isso repercutiu em alterações estéticas, suscetibilidade à infecção, problemas respiratórios (Aron & Crowe, 1985), dificuldades mastigatórias e importantes sinais clínicos associados ao mau funcionamento da drenagem lacrimal (Breit et al., 2003; Schlueter et al., 2009). Os animais afetados por essa condição, por possuírem o nariz externo ausente ou pouco desenvolvido, tendem a ter os pelos descoloridos ao redor dos olhos, devido ao excesso de lágrimas e interrupções do fluxo de drenagem lacrimal, diferentemente do que ocorre com os gatos mesocefálicos (Künzel et al., 2003).

Esta característica pode ser decorrente de um ducto nasolacrimal fino e tortuoso. Estudos com radiografias e moldes convencionais demonstraram que esse ducto nos gatos

braquicefálicos possui um trajeto em ângulo reto, ou mesmo em curso acutângulo, e em formato de "V", nos casos extremos, o que dificulta a drenagem das lágrimas pelo seio nasolacrimal até a narina externa. Como essas dismorfologias podem afetar o bem-estar dos animais e predispô-los a alterações funcionais, a seleção de formas braquicefálicas, especialmente as mais severas, devem ser reconsideradas (Kleiner et al., 2004; Schlueter et al., 2009; Schmidt, 2017).

Portanto, o reconhecimento fenotípico baseado em critérios morfológicos craniométricos pode contribuir para a nomenclatura dos formatos cranianos em felinos domésticos. Além disso, a descrição anatômica do trajeto de drenagem lacrimal nos gatos Persas facilitará o planejamento estratégico de abordagens clínicas ou cirúrgicas, melhorando a qualidade de vida desses animais.

1.1. Objetivos

1.1.1 Geral

- Caracterizar a morfometria craniana de gatos brasileiros de pelo curto (BSH) e da raça Persa;
- Descrever o trajeto do ducto nasolacrimal em felinos domésticos da raça Persa;

1.1.2 Específicos

- Aferir o Índice Craniano e o Ângulo Craniofacial de felinos domésticos com e sem focinho curto;
- Caracterizar o ducto nasolacrimal de gatos Persas, quanto ao trajeto, comprimento, diâmetro e sua relação com os ossos cranianos e a raiz do dente canino superior.

1.2. Justificativa

Os estudos morfométricos permitem a aquisição de dados que trazem contribuições científicas no estudo da influência genética e do ambiente no desenvolvimento dos indivíduos. Permitem também a obtenção de conhecimentos de anatomia clínica, aplicáveis na prática de medicina interna e cirúrgica, permitindo ao médico veterinário o conhecimento e visualização de detalhes anatômicos (Monfared, 2013). Além disso, serve de instrumental

para entendimento de como a braquicefalia se relaciona com componentes ambientais para o desenvolvimento individual (Wehausen & Ramsey, 2000).

A padronização da nomenclatura utilizada nas ciências médicas é fundamental tanto para a prática clínica quanto para a pesquisa científica. Além de facilitar a comunicação entre os profissionais e pesquisadores, aumenta a confiabilidade da comparação entre resultados de diferentes áreas, favorecendo um melhor nível de evidência científica.

A realização deste estudo contribuirá com a elucidação de particularidades anatômicas importantes para a prática clínica de Medicina Veterinária, como por exemplo, as influências do tipo craniano na realização de anestesias locais, particularidades como o sistema de drenagem nasolacrimal em gatos domésticos braquicéfalos e implicações funcionais da forma da cabeça felina (Künzel et al., 2003; Schlueter et al., 2009; Monfared, 2013). Finalmente, o reconhecimento do padrão anatômico do ducto nasolacrimal nos gatos Persa corrobora para o entendimento anatômico-funcional da drenagem lacrimal nesses animais, podendo servir de apoio a abordagens terapêuticas ligadas às patologias oftálmicas nesses animais.

2. REVISÃO DE LITERATURA

2.1 Crânio felino e seus fenótipos

O gato doméstico (*Felis catus*, Linnaeus, 1758) tem sua cabeça óssea dividida em crânio e face, compreendendo também a mandíbula e o hioide. A cabeça óssea define-se como um meio de proteção para o encéfalo e para os órgãos dos sentidos especiais como visão, olfato, audição, paladar e equilíbrio (Dyce et al., 2009; Nav, 2017).

Os ossos do crânio desenvolvem-se a partir de centros de ossificação independentes e têm, em sua maioria, homologias bem estabelecidas. Nos animais jovens estão separados uns dos outros por finas fibras de tecido conjuntivo fibroso, o que confere mobilidade suficiente para permitir o seu crescimento. Terminando o crescimento, a ossificação estende-se ao tecido conjuntivo e cartilagíneo, tornando imóveis as articulações localizadas entre a maioria dos ossos da cabeça óssea, denominadas suturas se associadas a tecido conjuntivo ou sincondroses se associadas ao tecido cartilagíneo. Este processo de ossificação muitas vezes não é completo, permitindo distinguir os contornos dos diferentes ossos cranianos, mesmo em animais geriátricos (Dyce et al., 2009).

A cabeça óssea pode ser separada em duas partes distintas, a caudal que envolve o encéfalo e a rostral que suporta a face. Na maioria dos animais domésticos a face é maior do que o crânio, encontrando-se rostralmente a este. Os ossos do crânio envolvem a cavidade craniana. Esta estrutura óssea é constituída por diversas unidades ósseas, cuja organização é bastante diferenciada nos diversos animais, sendo necessário ter em conta não só as espécies e as raças em causa, como também, a idade e o gênero (König & Liebich, 2002; Nav, 2017).

O crânio felino é constituído pelos ossos occipital, esfenoide, pterigoide, etmoide, vômer, temporal, parietal e frontal, que formam as paredes da cavidade craniana. Assim,

podemos observar o assoalho, que é constituído pela porção basilar do osso ímpar occipital e pelas duas partes do osso ímpar esfenoide; a parede nucal contempla a porção escamosa e porção lateral do osso ímpar occipital; as paredes laterais são formadas pelos ossos pares temporais; o teto que é formado pelos ossos pares frontais e parietais e a parede nasal apresenta o osso ímpar etmoide. Os gatos apresentam uma mandíbula globosa, arcos zigomáticos convexos e muito salientes e a face relativamente curta, correspondendo a aproximadamente 20% do comprimento total da cabeça (König & Liebich, 2002; Karan et al., 2006; Dyce et al., 2009; Nav, 2017).

A aparência fenotípica da cabeça de um felino depende da forma do crânio e é muito relacionado a especificidade de raças. Na literatura são poucos os estudos comparando os diferentes morfotipos de crânios em gatos. Na maioria dos gatos, a face é relativamente pequena. Porém, em certas raças orientais, como o Siamês, a cabeça é alongada, de forma triangular, terminando de uma forma mais suave e contrastando com os gatos de raça Persas, que possuem uma cabeça mais arredondada, curta, destacando-se a órbita, além de apresentarem redução dos ossos faciais (Wehausen & Ramsey, 2000; Dyce et al., 2009; Uddin et al., 2013).

2.2 Craniometria e nomenclatura craniana

A terminologia usada para descrever o diagnóstico craniofacial em medicina veterinária resultou da antropometria clássica, que emprega medidas tomadas em indivíduos vivos e crânios humanos, bem como índices que representam proporções faciais (Edler et al., 2006). O mais comum entre estes é o índice cranial, que classifica os tipos de crânio como braquicefálico, mesocéfalo e dolicocéfalo (Farkas, 1986). Com base em determinados pontos craniométricos e acidentes ósseos do crânio é possível estabelecer diversas medidas lineares. Estas medidas caracterizam as diferenças raciais e relacionam-se com o comprimento relativo da parte facial, o que permite que se possam identificar raças dolicocefálicas, braquicefálicas e mesaticefálicas (Regodón et al., 1993). Ainda não existem relatos de morfometria craniana para felinos domésticos que possam classificá-los segundo a forma craniana, existindo apenas um acordo entre os autores sobre o assunto, que atribui a essa espécie uma nomenclatura classificatória baseada apenas em critérios fenotípicos (Künzel et al., 2003; Schlueter et al., 2009).

O termo *braquicefálico* descreve a aparência com uma cabeça redonda e achatada na porção caudal. Está associado à fusão prematura da sutura coronal, causando um encurtamento do eixo occipitofrontal do crânio, encurtamento dos ossos craniofaciais, arcos zigomáticos pronunciados e com uma curvatura significativa do neurocrânio (Brehm et al., 1985; Evans, 1993; Drake & Klingenberg, 2010).

O ângulo craniofacial (CFA) e o Índice Cefálico (IC) são critérios importantes na classificação da forma craniana em cães (Regodón et al., 1993). O IC é a relação entre a largura e o comprimento do crânio, sendo que o comprimento do crânio é mensurado a partir da crista nucal até a extremidade rostral da sutura interincisiva; a largura craniana é a medida entre os ápices dos arcos zigomáticos; o IC é dado pela fórmula: IC = 100 x largura do crânio (distância entre os arcos zigomáticos) / comprimento do crânio (distância entre o íneo e o próstio). Nos cães dolicocefálicos, o índice é abaixo de 50, enquanto em cães braquicefálicos chega a valores próximos a 100. Não existem referências do IC para felinos domésticos. O CFA é o ângulo formado pelos eixos basilar e facial, sendo que o primeiro é conseguido unindo o osso basioccipital à margem caudal do sulco quiasmático; e o segundo é determinado pelo prolongamento caudal da projeção do palato duro. Um estudo anterior demonstrou a classificação craniana baseada no CFA, de radiografias de crânios caninos. Segundo seus resultados, cães braquicefálicos possuem ângulos craniofaciais entre 9^0 e 14^0, cães mesocefálicos entre 19^0 e 21^0, e galgos dolicocefálicos entre 25^0 a 26^0 (Regodón, 1988; Regodón et al., 1993). Estes dados não foram, até o momento, reportados em felinos domésticos.

2.3 Anatomofisiologia do aparelho lacrimal

O aparelho lacrimal é composto por dois componentes: o aparelho secretor e o aparelho excretor. O aparelho lacrimal excretor é composto por uma rede de condutos de parede fina que drena o filme lacrimal desde o olho à cavidade nasal. No que se refere à sua constituição, o aparelho secretor inclui a glândula lacrimal, a glândula da terceira pálpebra e as glândulas lacrimais acessórias. Estas, por sua vez, incluem as células caliciformes, as glândulas tarsais ou glândulas de Meibômio e as glândulas de Moll e de Zeiss. O reflexo de fechamento das pálpebras estimula a produção de secreção por estas glândulas, que se espalha uniformemente por toda a superfície da córnea. O aparelho de drenagem lacrimal consiste no ponto lacrimal superior e inferior, nos canalículos lacrimais superior e inferior, no saco

lacrimal, no ducto nasolacrimal e no óstio nasal (Roberts et al., 1974; Diesem 1981; Severin 1991; Habin 1993; Nöller et al., 2006).

A função principal do aparelho nasolacrimal é drenar o filme lacrimal desde a superfície do olho até o óstio nasal. A evaporação do filme lacrimal contribui também para a sua eliminação, podendo remover aproximadamente 25% da lágrima da superfície ocular, conforme condições atmosféricas. Cerca de 60% do volume lacrimal é drenado para o ponto lacrimal inferior e respectivo canalículo. As lágrimas fluem ventralmente em resposta à gravidade, entrando nos canalículos durante o fechamento palpebral, devido à redução da pressão intracanalicular. Esta redução de pressão decorre da contração do músculo orbicular, que comprime os ductos. Além disso, a ação capilar e o efeito sifão do saco lacrimal puxam a lágrima para o canalículo lacrimal e ducto nasolacrimal. Em animais domésticos o canalículo lacrimal inferior parece ser o mais importante no papel de drenagem do filme lacrimal (Grahn & Sandmeyer, 2013).

Os pontos lacrimais de drenagem da lágrima são aberturas ovais que medem aproximadamente 0,3 a 1 mm de diâmetro e estão localizados na conjuntiva palpebral do bordo das pálpebras superior e inferior e encontram-se aproximadamente 2 a 5 mm afastados do canto medial, aproximadamente onde as glândulas tarsais terminam. Em alguns animais, um ou os dois pontos lacrimais podem ter tamanhos diferenciados ou mesmo estarem ausentes (agenesia do ponto lacrimal), resultando em epífora (Grahn & Sandmeyer, 2013).

O canalículo lacrimal superior corre medialmente paralelo à margem palpebral, virando depois ventromedialmente desde a comissura das pálpebras até à entrada do saco lacrimal. O canalículo lacrimal inferior se direciona inframedialmente, desde o ponto lacrimal até se unir com o canalículo superior no saco lacrimal. Este fica contido na fossa lacrimal que é formada pelo osso lacrimal. O saco lacrimal é a origem do ducto nasolacrimal, sendo que nos felinos esse saco não é claramente delimitado do ducto nasolacrimal (Nöller et al., 2006).

O ducto nasolacrimal é irrigado por um ramo da artéria malar e pode ser subdividido em três partes: uma parte caudal, uma média e uma rostral. A porção proximal é rodeada por um canal ósseo que começa no forâmen lacrimal e alonga-se pelo osso maxilar. Na parte caudal da cavidade nasal, a lâmina basal constitui a parede medial do canal lacrimal, onde ele repousa amplamente contra a superfície interna do osso maxilar. A parte média do ducto nasolacrimal situa-se ventralmente à lâmina basal da concha nasal e é delimitado lateralmente pelo osso maxilar. Na parte cranial do ducto nasolacrimal a delineação dorsal da concha nasal ventral está ausente e o aspeto medial do ducto nasolacrimal é exclusivamente coberto por mucosa. Rostralmente, o ducto passa medial à cartilagem nasal ventrolateral e termina

abrindo-se no assoalho ventrolateral do vestíbulo nasal, ventral à dobra alar (Nöller et al., 2006; Evans & Lahunta, 2010). Os gatos braquicefálicos normalmente possuem ductos nasolacrimais curtos e drenam as lágrimas para a faringe, sendo descrita uma comunicação do ducto nasolacrimal com a cavidade nasal, ao nível da raiz do dente canino (Michel, 1955; Samuelson, 2013; Grahn & Sandmeyer, 2013).

2.4 Alterações oftalmológicas na braquicefalia

O estudo da braquicefalia em gatos é importante porque a forma do crânio do gato Persa tem sido associada a problemas oftalmológicos, faciais, dentários, respiratórios, neurológicos e reprodutivos, e essas condições podem ser mais graves em gatos com braquicefalia mais extrema (Farnworth et al., 2016; Schmidt et al., 2017). A manifestação da síndrome braquicefálica em gatos vai muito além dos graves problemas respiratórios. Dificuldades mastigatórias em função de má oclusão dentária, fissuras labial e palatina, tumores intracranianos, epífora, exoftalmia, lagoftalmia, triquíase e entrópio do canto medial, ceratoconjuntivite seca (CCS), ceratite pigmentar, úlceras de córnea, predisposições a traumas oculares e bloqueio dos ductos lacrimais (Hayes et al., 1975; Aron & Crowe 1985; Breit et al., 2003; Schlueter et al., 2009; Williams et al., 2012; Labelle et al., 2013).

A conformação anatômica da órbita e crânio dos animais braquicefálicos propicia a exposição exacerbada do bulbo ocular. Em adição, a sensibilidade corneal nesses animais pode ser reduzida comparativamente às raças não braquicefálicas, devido à inervação reduzida na superfície corneal, contribuindo para úlceras recorrentes ou ceratites ulcerativas (Blocker & van der Woerdt, 2001; Hamor, 2007; Kafarnik et al., 2008).

Além disso, essa conformação craniana com ossos faciais reduzidos contribui para a epífora, que se manifesta através do extravasamento de lágrimas dos olhos. As causas mais comuns estão relacionadas à insuficiência do sistema nasolacrimal, estenoses e bloqueios dos ductos nasolacrimais além de síndromes que resultam na produção excessiva de lágrimas. Nos gatos Persas, o ducto nasolacrimal pode ser tortuoso, os pontos lacrimais inferiores podem estar deslocados ventralmente ou até não estar presentes (atresia), dificultando a drenagem da lagrima, e colaborando para dermatite das pregas nasais (Roberts, 1962; Carwardine, 1976; Gerding, 1991; Breit et al., 2003; Gelatt, 2003).

O Teste de Jones avalia a patência do ducto nasolacrimal, utilizando-se um corante vital (fluoresceína) no saco conjuntival e, posteriormente, a observação do seu aparecimento

na saída do vestíbulo nasal, na narina ipsilateral, confirmando a permeabilidade do ducto. O intervalo requerido para que a fluoresceína apareça é muito variável em cães e gatos e está dependente de muitos fatores, como o comprimento do focinho, a conformação do crânio. Em cães, a média do tempo de trânsito normal da passagem da fluoresceína é aproximadamente 4 minutos, mas varia entre 35 segundos a 30 minutos. Em gatos, a média do tempo de passagem varia de 46 segundos, até um tempo superior a 30 minutos ou mesmo não ocorrer (Küpper, 1973; Cullen & Grahn, 2003; Ota et al., 2009; Zemljič et al., 2011; Maggs et al., 2013; Dawson et al., 2015).

A dacriocistografia é um exame de imagem, que avalia o ducto nasolacrimal após a aplicação do meio de contraste. Esse processo permite a localização de obstruções parciais ou completas do ducto, além da visualização de dilatações, desvios, constrições do ducto, e agenesia dos canais lacrimais (Küpper, 1973; Spiess & Pot et al., 2013). Foi originalmente descrita como uma técnica radiográfica, mas atualmente a tomografia computadorizada combina as imagens bidimensionais e tridimensionais reconstituídas e realiza o realinhamento por contraste do aparelho lacrimal (Gelatt, 2003; Kanski 2004a, 2004b).

Na apresentação radiográfica dos ductos lacrimais (dacriocistografia) do gato, os sacos lacrimais ficam preenchidos com meio de contraste e se apresentam como sombreamento. Na vista radiográfica laterolateral, o ducto nasolacrimal se projeta a meio caminho entre os ossos nasal e palatino, ficando sobreposto pelo labirinto etmoidal, pela concha nasal ventral, pelos ductos nasofaríngeos e pelo osso maxilar. Para identificação do ducto nasolacrimal, a partir do saco lacrimal, o mesmo descola ligeiramente para o bordo maxilar superior, ao longo do vértice do dente canino. Sua porção mais curta, descendente, se estende na direção ventral, tendo o seu curso adicional dependente da forma do crânio (Küpper, 1973; Breit et al., 2003). Em raças braquicefálicas, o ângulo formado entre os ramos ascendente e descendente do canal nasolacrimal está proporcionalmente relacionado com a redução do esqueleto facial. Este curso agudo pode dificultar a drenagem da lágrima (Nöller et al., 2006).

A possibilidade de realizar reconstruções em três dimensões pós-processamento das imagens tem um papel importante, pois elimina a limitação radiográfica associada à sobreposição de estruturas (Thrall, 2013). Além disso, os aparelhos tomográficos modernos permitem fazer aquisição de imagens com elevada resolução, cortes finos e excelentes visualizações de detalhes dos acidentes ósseos. Finalmente, aos algoritmos modernos utilizados no pós-processamento de imagem, permitem reconstruções tridimensionais com

reduzido tempo de aquisição. Estas características indicam a tomografia computorizada como um ótimo meio de avaliação da conformação do crânio (Schwarz et al., 2002).

3. REFERÊNCIAS BIBLIOGRÁFICAS

ARON, D. N.; & CROWE, D. T. Upper Airway Obstruction General Principles and Selected Conditions in the Dog and Cat. **Veterinary Clinics of North America: Small Animal Practice**, v. 15, n. 5, p. 891–917, 1985.

BERTOLINI, F.; GANDOLFI, B.; KIM, E. S.; et al. Evidence of selection signatures that shape the Persian cat breed. **Mammalian Genome**, v. 27, n. 3-4, p. 144–155, 2016.

BLOCKER, T.; VAN DER WOERDT, A. A comparison of corneal sensitivity between brachycephalic and Domestic Short-haired cats. **Veterinary Ophthalmology**, v. 4, n. 2, p. 127–130, 2001.

BREHM, H.; LOEFFLER, K.; KOMEYLI, H. Schädelformen beim Hund. **Anatomia Histologia Embryologia**, v. 14, n. 1, p. 324–331, 1985.

BREIT, S.; KÜNZEL, W.; OPPEL, M. The course of the nasolacrimal duct in brachycephalic cats. **Anatomia Histologya Embryologya**, v. 32, p. 224–2271, 2003.

CARWARDINE, P. C.; TEMPLETON, R. Excessive lachrymation in the dog. **The Veterinary Record,** v. 98, n. 10, p. 245-246, mar. 1976.

CONSTANTINESCU, G. M. **Anatomia clínica de pequenos animais**. Rio de Janeiro: Guanabara Koogan, 2005. 355 p.

CULLEN, C. L.; GRAHN, B. H. Diagnostic ophthalmology. Congenital medial canthal cyst. The Canadian Veterinary Journal. **La Revue Vétérinaire Canadienne**, v. 44, n. 11, p. 935–937, 2003.

DAWSON, C.; DIXON, J.; LAM, R.; PRIESTNALL, S. L.; SCANILLA, N. Differential diagnoses, investigation, and management of a periocular swelling close to the nasolacrimal duct in a horse - A case report of Dacryops. **Veterinary Ophthalmology**, v. 19. N. 5, p. 427–431, 2015.

DIESEM, C. Generalidades sobre órgãos sensoriais e tegumento comum: o órgão da visão, In: Getty R. (Ed.), Sisson & Grossman. **Anatomia dos Animais Domésticos**. Vol.1. 5ª ed. Interamericana, Rio de Janeiro, p. 207-222, 1981.

DONE, S. H.; GOODY, P. C. & EVANS, S. A. A**tlas Colorido de Anatomia Veterinária do cão e do gato**, 2nd ed. Elsevier, 1990.

DRAKE, A. G.; KLINGENBERG, C. P. Large-scale diversification of skull shape in domestic dogs: disparity and modularity. **The American Naturalist**, v. 175, n. 3. p. 289–301, 2010.

DYCE, K. M., SACK, W.O. & WENSING, C.J.G. The locomotor apparatus, the nervous system, the head and ventral neck of the dog and cat. In: Dyce, K.M., Sack, W.O., Wensing, C. J. G. (Eds.) **Textbook of Veterinary Anatomy**. Elsevier Health Sciences, St. Louis, Missouri, pp. 57, 59, 62, 63, 306, 307, 376, 2009.

EDLER, R.; AGARWAL, P.; WERTHEIM, D.; GREENHILL, D. The use of anthropometric proportion indices in the measurement of facial attractiveness. **European Journal of Orthodontics**, v. 28, n. 3, p. 274-281, 2006.

EVANS, H. E.; LAHUNTA, A. **Guide to the dissection of the dog**, 7th ed., Missouri: Saunders Elsevier, 2010.

EVANS, H. E.; The skeleton. In: **Millers' anatomy of the dog**. Hrsg. H. E. Evans, W. B. Saunders Company, Philadelphia, p.122-218, 1993.

FARKAS, L.G.; MUNRO, I. R. Anthropometric facial proportions in Medicine. **Springfield**: Charles C. Thomas Publisher, 1986.

FARNWORTH, M. J.; CHEN, R.; PACKER, R. M. A.; CANEY, S. M. A. & GUNN-MOORE, D. A. Flat feline faces: Is brachycephaly associated with respiratory abnormalities in the domestic cat 'felis catus'? **PLoS ONE** v.11, n.8, 2016.

GANDOLFI, B.; ALHADDAD, H.; AFFOLTER, V.K.; BROCKMAN, J. et al. To the root of the curl: a signature of a recent selective sweep identifies a mutation that defines the cornish rex cat breed, **PLoS One**, v. 8 n. 6, 2013.

GELATT, K. N. Doenças e cirurgia do sistema lacrimal e nasolacrimal do cão. In: ____. **Manual de oftalmologia veterinária**. São Paulo: Manole, p.73- 94, 2003.

GERDING JR., P. A. Epiphora associated with canaliculus in a dog. **Journal of the American Animal Hospital Association,** v. 27, n. 4, p. 424-426, 1991.

GRAHN, B.; SANDMEYER, L. Diseases and Surgery of the Canine Nasolacrimal System. In: Gelatt, K. N. (Ed.). **Veterinary Ophthalmology**, 5th edition. Wiley Blackwell, Ames, Iowa, USA, 894–911, 2013.

HABIN, D. The nasolacrimal system, In: Petersen-Jones S.M. & Crispin S.M. (Eds), **Manual of Small Animal Ophthalmology**. Brit. Small Anim. Vet. Assoc., Shurdington, p. 91-102, 1993.

HAMOR, R. E. Terceira pálpebra. In: SLATTER, D. **Manual de cirurgia de pequenos animais**. 3º Edição. São Paulo: Manole, p. 1361-1368, 2007.

HAYES, H. M.; PRIESTER, W. A; PENDERGRASS, T. W. Occurrence of nervous tissue tumors in cattle, horses, cats and dogs. **Internacional Journal Cancer**, vol.15, n.1, p. 39–47, 1975.

KAFARNIK, C.; FRITSCHE, J.; & REESE, S. Corneal innervation in mesocephalic and brachycephalic dogs and cats: assessment using in vivo confocal microscopy. **Veterinary Ophthalmology**, v. 11, n. 6, p. 363–367, 2008.

KANSKI, J. J. Distúrbio do sistema de drenagem lacrimal, In: Ibid. (Ed.), **Oftalmologia Clínica: uma abordagem sistemática**. 4ª ed. Revinter, Rio de Janeiro, p. 43-54, 2004a.

KANSKI, J. J. Sistema de drenagem lacrimal, p.43-55. In: Ibid. (Ed.), **Oftalmologia Clínica: uma abordagem sistemática**. 5ª ed. Elsevier, Rio de Janeiro, p. 43-55, 2004b.

KARAN, M.; TIMURKAAN, S.; OZDEMIR, D. O.; UNSALDI, E. U. Comparative Macroanatomical Study of the Neurocranium in some Carnivora. **Anatomia Histolologia Embryologia**, v. 35, n. 1, p. 53–56, 2006.

KIM, E.S.; SONSTEGARD, T. S.; ROTHSCHILD, M.F. Recent artificial selection in US Jersey cattle impacts autozygosity levels of specific genomic regions. **BMC Genomic**, v.16, p. 302, 2015.

KLEINER, J. A.; WOUK, A. F. P.; COSTA, P. V.; FIDELCINO, A. A dacriocistorrinografia em cães e gatos. Medvep, **Revista Científica de Medicina Veterinária**, v. 2, n. 7, p. 185-189, 2004.

KÜNZEL, W.; BREIT, S.; OPPEL, M. Morphometric investigations of breed-specific features in feline skulls and considerations on their functional implications. **Anatomia Histolologya Embryologya,** v. 32 p. 218-23, 2003.

KÖNIG, H. E. & LIEBICH, H. G. Anatomia dos Animais Domésticos: Texto e Atlas Colorido. Vol.1. Artmed, Porto Alegre. 2002. 262p.

KÜPPER, W. Die darstellung des tränennasenganges bei der katze. **Kleintierpraxis,** v. 18, p. 42–4, 1973.

KURUSHIMA, J. D.; LIPINSKI, M. J.; GANDOLFI, B.; FROENICKE, L.; et al. Variation of cats under domestication: genetic assignment of domestic cats to breeds and worldwide random-bred populations. **Animal Genetics**, v. 44, n. 3, p. 311–324, 2012.

LABELLE, A. L.; DRESSER, C. B.; HAMOR, R. E.; ALLENDER, M. C.; et al. Characteristics of, prevalence of, and risk factors for corneal pigmentation (pigmentary keratopathy) in pugs. **Jounal American Veterinarian Medical Association**, vol. 243, p. 667-674, 2013.

LIPINSKI, M. J.; FROENICKE, L.; BAYSAC, K. C.; BILLINGS, N. C.; et al. The ascent of cat breeds: Genetic evaluations of breeds and worldwide random-bred populations. **Genomics**, v. 91, n. 1, p. 12–21, 2008.

MAGGS, D.; MILLER, P.; OFRI, R. **Slatter's Fundamentals of Veterinary Ophthalmology**. Elsevier Health Sciences, 2013.

MICHEL, G. Beitrag zur Anatomie der Tränenorgane von Hund und Katze. Deutsche. **Tierärztliche Wochenschrft**, v. 62, p. 347–349, 1955.

MONFARED, A. L. Clinical anatomy of the skull of Iranian native sheep. **Global Veterinaria**, v.10, n. 3, p. 271-275, 2013.

NÖLLER, C.; WOLFGANG, H.; DIETRICH, H. W.; GRÖNEMEYER, R. M.; et al. Computed tomography-anatomy of the normal feline nasolacrimal drainage system. **Veterinary Radiology & Ultrasound**, v. 47, n. 1, p. 53–60, 2006.

NOMINA ANATOMICA VETERINARIA (NAV). **International Committee on Veterinary Gross Anatomical Nomenclature**. 6. Ed. Hanover (Germany), Ghent (Belgium), Columbia, MO (U.S.A.), Rio de Janeiro (Brazil), 2017.

OTA, J.; PEARCE, J. W.; FINN, M. J.; JOHNSON, G. C.; GIULIANO, E. A. Dacryops (lacrimal cyst) in three young labrador retrievers. **Journal of the American Animal Hospital Association**, v. 45, n. 4, p. 191–196, 2009.

PARKER, H. G.; KIM, L. V.; SUTTER, N. B.; et al. Genetic structure of the purebred domestic dog. **Science**, v. 304, n. 5674, p. 1160-1164, 2004.

POLLINGER, J. P.; BUSTAMANTE, C. D.; FLEDEL-ALON, A.; SCHMUTZ, S.; et al. Selective sweep mapping of genes with large phenotypic effects. G**enome research,** vol. 15, n. 12, p. 1809–1819, 2005.

REGODÓN, S. Estudio de los parametros topograficos craneoencefalofaciales del galgo, pointer y Pequines en base a metodos radiológicos y bioestatísticos. Tesis Doctorado. **Fac. Veterinary. Caceres**, 1988.

REGODÓN, S.; VIVO, J. M.; FRANCO, A.; GUILLÉN, M. T.; ROBINA, A. Craniofacial angle in dolichol, meso and brachycephalic dogs: radiological determination and application. Department of Anatomy and Embryology, Faculty of Veterinary Medicine, University of Extremadura, Spain. **Annals of Anatomy,** vol.175: p. 361-363, 1993.

ROBERTS, S. R. Abnormal tear secretion in the dog. **Modern Veterinary Practice**, v. 43, n. 37, p. 77, 1962.

ROBERTS, S. R.; VIERHELLER, R. C.; LENNOX, W. J. Eyes, In: Archibald J. (Ed.), **Canine Surgery**. 2nd ed. American Veterinary Publications, Santa Barbara, p. 193-262, 1974.

SAMUELSON, A. Ophthalmic Anatomy. In: Gelatt, K. N. (Ed.). **Veterinary Ophthalmology**, 5th edition. Wiley Blackwell, Ames, Iowa, USA, 39–170, 2013.

SCHLUETER, C.; BUDRAS, K. D.; LUDEWIG, E.; et al. Brachycephalic feline noses. CT and anatomical study of the relationship between head conformation and the nasolacrimal drainage system. **Journal Feline Medicine Surgery**, v. 11, p. 891–900, 2009.

SCHMIDT, M. J.; KAMPSCHULTE, M.; ENDERLEIN, S.; GORGAS, D.; et al. The Relationship between Brachycephalic Head Features in Modern Persian Cats and Dysmorphologies of the Skull and Internal Hydrocephalus. **Journal of Veterinary Internal Medicine**, v. 31, n. 5, p. 1487–1501, 2017.

SCHWARZ, T.; WELLER, R.; DICKIE, A. M.; KONAR, M.; et al. IMAGING OF THE CANINE AND FELINE TEMPOROMANDIBULAR JOINT: A REVIEW. **Veterinary Radiology Ultrasound**, v. 43, n. 2, p. 85–97, 2002.

SEVERIN, G. A. Aparato lacrimal. In: Ibid. (Ed.), **Manual de Oftalmologia Veterinária**. Hemisfério Sur, Buenos Aires, p. 85-97, 1991.

SPIESS, B. M.; POT, S. A. Diseases and Surgery of the Canine Orbit. In: Gelatt, K. N. (Ed.). **Veterinary Ophthalmology**, 5th edition. Wiley Blackwell, Ames, Iowa, USA, 793–831, 2013.

THRALL, D. E. **Textbook of Veterinary Diagnostic Radiology**, 6th edition, St. Louis: Saunders Elsevier, 2013, 864p.

UDDIN, M.; SARKER, M. H. R.; HOSSAIN, M. E.; ISLAM, M. S.; et al. Morphometric investigation of neurocranium in domestic cat (*Felis catus*). **Bangladesh Journal of Veterinary Medicine**, v. 11, n. 1, p. 69-73, 2013.

WEHAUSEN, J. D.; & RAMSEY, R. R. Cranial morphometric and evolutionary relationships in the northern range of ovis canadensis. **Journal of Mammalogy**, v. 81, n. 1, p. 145–161, 2000.

WILLIAMS, D., MIDDLETON, S., FATTAHIAN, H., MORIDPOUR, R. Comparison of hyaluronic acid-containing topical eye drops with carbomer-based topical ocular gel as a tear replacement in canine keratoconjunctivitis sicca: a prospective study in twenty five dogs. **Veterinarian Resident Forum**, vol. 3, p.229-232, 2012.

ZEMLJIČ, T.; MATHEIS, F. L.; VENZIN, C.; MAKARA, M.; et al. Orbito-nasal cyst in a young European short-haired cat. **Veterinary Ophthalmology**, v. 14, p. 122–129, 2011.

ZHAO, X.; ONTERU, S. K.; PIRIPI, S.; THOMPSON, K, G.; et al. In a shake of a lamb's tail: using genomics to unravel a cause of chondrodysplasia in Texel sheep. **Animal Genetics**, v. 43, p.9–18, 2012.

CAPITULO 2

CRANIOFACIAL ANGLE AND CRANIAL INDEX MEASURED BY CT SCAN IN CATS

1. ABSTRACT

The objective of this study was to measure the craniofacial angle (CFA) and the cranial index (CI), through computed tomography of the skull of cats with a short or long snout. In this study, Brazilian Shorthair (BSH) and Persian cats were compared with regard to cranial phenotype. The craniometric measurements used were cranial length (distance between the inion and nasion) and cranial width (distance between the zygomatic arches). CI was the ratio of cranial width to length, while CFA was the angle formed by the basilar and facial axes. The basilar axis was determined by the union of the basioccipital bone to the caudal margin of the chiasmatic sulcus, and the facial axis was determined by the caudal extension of the hard palate projection. Mean CI and CFA values for BSH and Persians were 61.7 and 78.7% and 12.0 and 9.1°, respectively. Only two cranial types were confirmed on the basis of the association of the two craniometric parameters (CI and CFA): brachycephalic, in Persian cats and non-brachycephalic, in BSH cats. These reference values for cats with a long nose and short nose (Persian) were determined in an unprecedented way, and could be used for the phenotypic classification of cat skulls.

Keywords: Brachycephaly, Cats, Cranial index, Craniofacial angle, Mensurement of cranial index.

2. INTRODUCTION

Craniometry consists in determing various linear measures based on specific craniometric points and bone charateristics of the skull. These parameters characterize the differences between cat breeds and allow their classification as dolicocephalic, mesocephalic and brachycephalic (Evans & Christensen, 1993). According to Hendricks (1992), dogs with a mean cranial index (CI) of 39% are characterized as dolichocephalic, whereas mesocephalic have a mean CI of 52% and brachycephalic of 81%.

Brachycephaly is one of the most easily recognizable phenotypic characteristics responsible for morphological changes in a substantial proportion of dogs and cats breeds (Bannasch et al., 2010). According to Pollinger et al. (2005), this characteristic derives from a skeletal mutation that changes the growth of the basilar portion of the occipital bones and the basophenoid bone, causing a premature fusion of the coronal suture, resulting in a shortening of the occipitofrontal axis and thereby a facial conformation with a short or flat nose.

This phenotype has been related to pathogenic syndromes such as respiratory and masticatory anomalies, cleft lip and palate, and ophthalmological diseases such as epiphora, exophthalmia, lagophthalmia, trichiasis and medial entropion, besides predisposing to keratoconjunctivitis sicca, pigmented keratitis, corneal ulcers and ocular trauma, among others (Hayes et al., 1975; Williams et al., 2012; Labelle et al., 2013). It has been suggested that the genetic selection of brachycephalic animals should be questioned, since high degrees of brachycephaly are also associated with malformations of the skull cap and facial and dental bones, which affect animal welfare (Schmidt et al., 2017).

The degree of brachycephaly in cats is evaluated subjectively using cranial morphology, due to the absence of morphometric data for classification in this specie (Schlueter et al., 2009). This evaluation has been made on the basis of cranial criteria of cats with only a short nose (Künzel et al., 2003), without anatomical dimensions and proportions of the skull objectively characterized in the literature (Wehausen & Ramsey, 2000; Uddin et

al., 2013). This led to four categories of brachycephaly being defined (Schlueter et al., 2009) based solely on phenotypic appearance, but without cranial morphometry to support this classification. Therefore, objective and solidified knowledge in statistical models corroborates to support the degrees of brachycephaly in cats (Schlueter et al., 2009).

According this, the objective of this study was to measure the craniofacial angle (CFA) and cranial index (CI) in adult Persian and Brazilian shorthair (BSH) cats by computed tomography (CT) to aid in the morphometric characterization of skulls of brachycephalic and non-brachycephalic cats.

3. MATERIALS AND METHODS

Thirty adult cats, males (n=14) and females (n=16), were divided into two groups. One group consisted of 20 cats of the BSH breed, weighing between 2 and 6 kg, which had died for reasons not related to the research, whereas the other group consisted of 10 Persian cats with weights between 3 and 6 kg. In the latter group, three live animals were used, coming from veterinary clinics (with the permission of the owner), and seven cadavers, which also died due to other reasons not relate to the research.

CT scans were performed using a single-detector row CT unit (General Electric, HiSpeed LXI, General Electric Medical Systems, Milwaukee, WI, USA). The cats were placed in the ventral decubitus position to obtain lateral and ventrodorsal topograms of the skull, used to evaluate correct positioning and for collimation of the region of interest, as well as for orientation of the two mm-thick transverse and perpendicular sections of the hard palate. For 3D imaging, all acquired images were then retroprojected in the bone algorithm in the CT software (window level between 200 and 2250 HU with bone filter to reduce noise), with standardized image format by the DICOM system.

The anatomical points considered for determining the linear measurements were: inion, nasion, and zygomatic arches. In each reference point, the linear craniometric measurements were obtained according to the length and the cranial width, represented by the distances between the inion and nasion, and between the zygomatic arches, respectively. The cranial index (CI) was then determined as the relation between these linear measurements, following the formula CI = 100 x skull width/skull length.

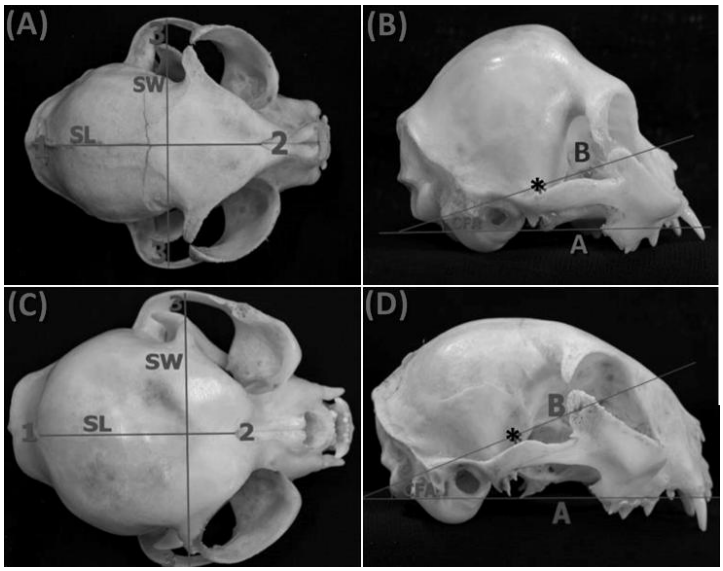

Figure 1. Dorsal macrophotograph of cat skulls with short (A) and long (C) snout showing reference anatomical points and linear measurements. SL = skull lengt; SW = skull width. Lateral views of macrophotographs of cat skulls with long (B) and short snout (D) showing determination of craniofacial angle (CFA); A: basilar axis; B: facial axis; (asterisk) chiasmatic sulcus site. 1= Inion; 2= Nasion; 3= zygomatic arch.

CFA was obtained as the angle formed by the basilar and facial axes, as proposed by Regodón et al. (1993). In this case, the basilar axis was obtained by union of the basioccipital bone with the caudal margin of the chiasmatic sulcus, while the facial axis was determined by the caudal extension of the projection of the hard palate (Figure 1). To mitigate the margin of error of the analysis, three measurements of each parameter studied (CFA and CI) were taken, always by the same examiner, and the average was used as the final value of the parameter analyzed. All the measurements were performed using DICOM image processing software (RadiAnt DICOM Viewer, version 3.4.2.13370), using the bone filter with a range between 200 and 1000 HU to optimize the contrast.

This study was submitted to the Ethics Committee on Animal Use of the University of Brasília and approved under Protocol No. 66690/2016.

Statistical analysis

Analysis of variance (ANOVA) was performed for the weight variable according to a completely randomized design with a 2 x 2 factorial arrangement (nose size: short and long, and sex: female and male). For the other variables, CFA and IC, ANOVA was also performed using the same design, including weight as a covariable in the model. Subsequently, a descriptive analysis was conducted to study the behavior of the variables according to the ANOVA results.

Pearson's correlation and regression analyses were performed to check associations between the variables studied. Linear and quadratic models were tested in the regression analysis, choosing the model that best fit the data.

Analyses of variance, descriptive, correlation and regression were respectively performed using the MIXED, MEANS, CORR and GLM procedures of Statistical Analysis System version 9.2 (SAS Inst. Inc., Cary, NC, USA). In the analyses done, $P \leq 0.05$ was considered significant. In ANOVA, least mean squares and standard errors were presented for the variables.

4. RESULTS

Males had CI values higher (P<0.05) than females, regardless of snout size (Table 1). This finding was not related to the weight of the animals, since in the statistical model, the CFA and CI variables were adjusted for weight, being considered a covariate. There was an interaction between nose size and sex (P<0.05) in weight of the cats (Table 1 and Figure 3). A nose size effect was detected (P<0.05) for CFA and CI, whereas a sex effect was observed (P<0.05) only for CI (Table 1).

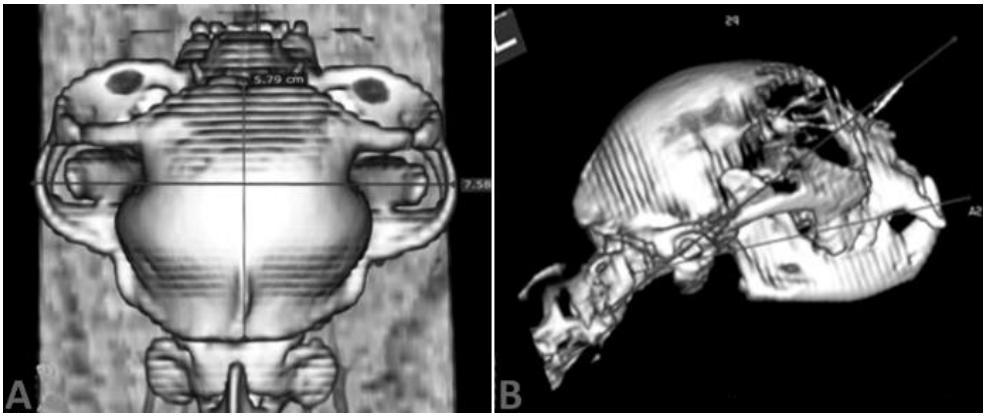

Figure 2. Ilustrative tomographic images of craniometric measurements, linear (A) and angular (B), through 3D reconstruction, using DICOM Viewer software.

Table 1. Effect of snout size and sex on weight, craniofacial angle (CFA) and cranial index (CI) of domestic cats

Variable	Snout size (SS)		Sex (S)		Source of variation		
	Short	Long	Female	Male	SS	S	SS × S
Weight (kg)	4.1 (0.24)	4.0 (0.17)	4.4 (0.21)	3.8 (0.21)	0.7165	0.0595	0.0391
CFA (°)	9.0 (0.33)^{b}	12.1 (0.24)^{a}	10.3 (0.29)	10.8 (0.30)	<0.0001	0.2340	0.8062
CI (%)	78.7 (1.00)^{a}	61.8 (0.71)^{b}	68.0 (0.88)^{B}	72.5 (0.92)^{A}	<0.0001	0.0020	0.0632

Least squares means (standard error). ^{a,b}Means followed by different lowercase letters between the snout sizes differ significantly (P<0.05) by the *F* test. ^{A,B}Means followed by different uppercase letters between the sexes differ significantly (P<0.05) by the *F* test.

Among the long-nosed cats, females were found to be heavier (P<0.05) than males, but this difference was not observed (P>0.05) in short-nosed animals (Figure 3). In turn, weight between short-nosed and long-nosed cats did not differ (P>0.05) in both sexes. The average CI found in Persian cats was 78.7%, while in long-nosed cats (BSH) was 61.7%.

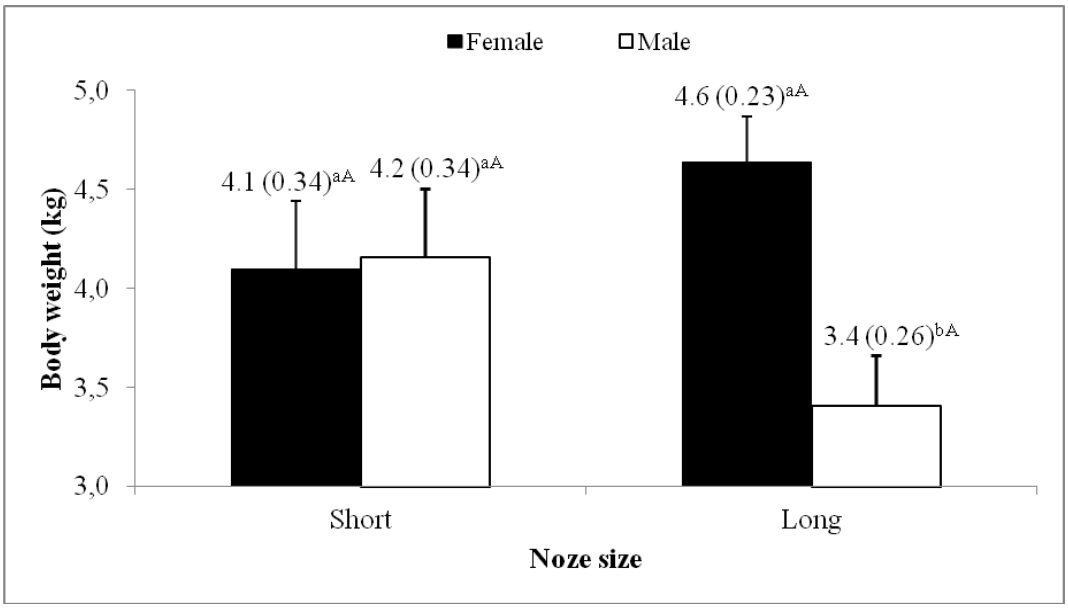

Figure 3. Schematic representation of the interaction between nose size and sex on the weight of domestic cats (P=0.0391). [a,b]Means followed by different lowercase letters between sexes within the same snout size differ significantly (P<0.05) by the *F* test. [A,B]Means followed by different uppercase letters between snout sizes within the same sex differ significantly (P<0.05) by the *F* test.

A descriptive analysis was performed for the variables weight, CFA and CI, according to nose size and sex (Table 2). Females had a higher coefficient of variation (CV) than males with either short (Persian) and long (BSH) noses for the variable weigth. On the other hand, the CV for CI was similar between females and males, regardless of nose size. In addition, the CV of CFA and CI for cats with short nose was higher than that obtained for cats with long nose.

Table 2. Descriptive analysis for weight, craniofacial angle (CFA) and cranial index (CI) of domestic cats

Variable	Snout size	Sex	N	Mean	SD	CV (%)	Minimum	Maximum
Weight (kg)	Short	Female	5	4.1	0.71	17.4	3.6	5.3
	Short	Male	5	4.2	0.26	6.3	3.9	4.5
	Long	Female	11	4.6	1.05	22.5	2.4	6.0
	Long	Male	9	3.4	0.50	14.7	2.8	4.2
CFA (°)	Short	Both	10	9.1	1.52	16.8	6.9	11.1
	Long	Both	20	12.0	0.70	5.8	11.0	13.1
CI (%)	Short	Both	10	78.7	5.72	7.3	64.5	84.6
	Long	Both	20	61.7	2.80	4.5	56.4	67.8
	Both	Female	16	64.9	8.00	12.3	56.4	79.5
	Both	Male	14	70.2	9.61	13.7	60.0	84.6

N = number of animals; SD = standard deviation; CV = coefficient of variation.

In the correlation analysis, weight showed no correlation ($P>0.05$) with CFA and CI. On the other hand, we saw that CFA was inversely correlated ($P<0.05$) with CI, demonstrating that as CFA increases, CI decreases, in both sexes.

To corroborate the correlation analysis, regression analysis was performed, where linear and quadratic models were tested (Figure 4). We confirmed that weight of the cats had little influence on CFA ($R^2=0.0087$) and CI ($R^2=0.1757$). The quadratic model explained better the variability of the CI as a function of weight when compared to the linear model ($R^2=0.0159$; data not shown), giving a valid equation ($P<0.05$): $CI=7.90+30.54*WEIGHT-3.74*WEIGHT^2$. CFA influenced reasonably the variability of CI ($R^2=0.4136$), in which the valid linear equation ($P<0.05$) $CI=103.84–3.30*CFA$ showed that brachycephalic cats with a broad skull (higher CI) have lower CFA values. These equations allowed us to determine CI values as a function of both the weight and CFA of the animal.

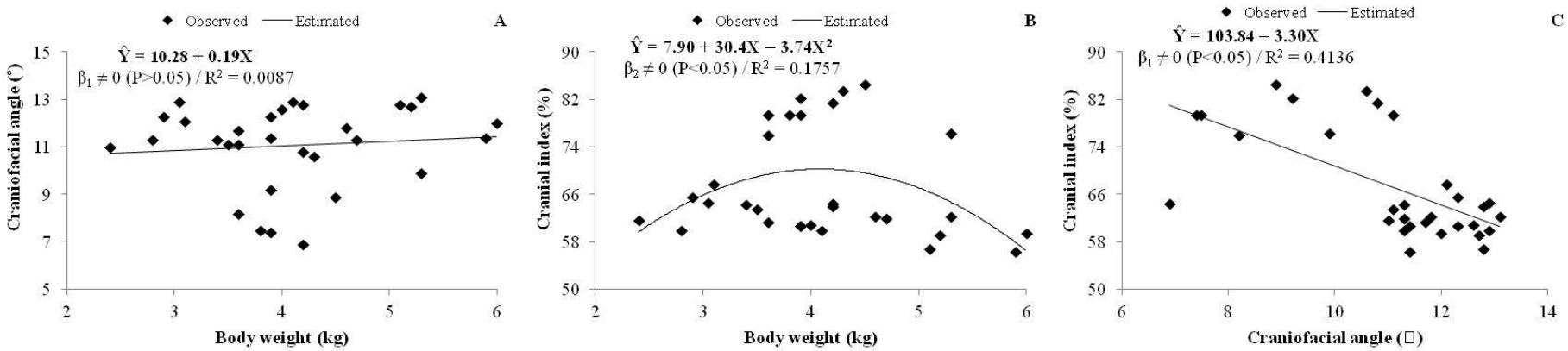

Figure 4. Regression analysis between craniofacial angle and weight (A), cranial index and weight (B), and cranial index and craniofacial angle (C) in domestic cats (grouped data).

5. DISCUSSION

In this study we observed that males had higher CI values than females, which can be explained due to sexual dimorphism, according to another study conducted with dogs, in which males had longer and wider skulls compared to females (Christiansen & Harris, 2012; Steffen & Heidecke, 2012; Uddin et al., 2014).

Although the study sample showed small variability related to the weight of the animals, that fact did not have significant influence on the results of CI and CFA, by regression analysis. The higher variability of CFA and CI (table 2) in short-nosed cats in this study reinforces the previous four categories classification of short-nosed cats, according to the extent of phenotypically abnormalities and craniofacial variations (Schlueter et al., 2009).

According to the literature, cats with a long nose are classified as mesocephalic or dolichocephalic. Due to the methodology employed in the present study, it is reasonable to assume that the BSH cats should be classified as non-brachycephalic only, since there was no statistical support to distribute them into wedge-shaped and triangular skull, as reported previously by Künzel et al. (2003), neither into brachycephalic and dolichocephalic, as described by Evans & Christensen (1993).

Previous studies were analyzed as a comparative support for classifying our results. Australian short-nosed domestic cats were classified as brachycephalic with an average CI of 71.1% (Saber et al., 2016). The Pekingese breed was identified as brachycephalic, with an average CI of 81% (Evans & Christensen, 1993). The average CI found here was 78.7%, close to the previously mentioned studies on Persian cats and Pekingese dogs, reinforcing that this sample can also be classified as brachycephalic. German Shepherd and Beagle breeds were classified as mesocephalic, based on an average CI of 52% (Saber et al., 2016), results consistent with the long-nosed cats in this study (BSH IC = 61, 7%). As we did not find

consistent difference that could classify this samples between dolico and mesocephalic, the authors preferred to refer to these animals as non-brachycephalic or long-nosed cats.

The mean value of 61.7% for the CI of long-nosed cats (BSH) in our study was higher than the CI described for European long-nosed cats (European short hair), classified as mesocephalic (Künzel et al., 2003). However, the same author described the mean CI of 58 and 60% for BSH and Siamese cats, which were classified respectively as mesocephalic and dolichocephalic. Thus, in the literature, there are disagreements between the authors regarding the classification of animals with long noses. Due to the lower variability of CI and CFA for long-nosed cats (BSH) in the present study, it would be reasonable to consider these cats to be non-brachycephalic only.

Feline skull morphometry confirmed that brachycephalic skulls are quite heterogeneous (Künzel et al., 2003), as well as brachycephaly phenotypes in dogs (Koch et al., 2012). The differentiation between CFA-based brachycephalic, mesocephalic, and dolichocephalic (Regodón et al., 1993) has been questioned for some races because it does not meet the goal (Koch et al., 2012). In the BSH and Persian cats of this study, CFA was adequate to differentiate brachycephalic from non-brachycephalic, but do not statistically support the differentiation in meso and dolichocephalic, due to the small variability of CFA.

A study evaluating European domestic cats in three different stages of life (<6 months, 6 to 11.5 months and >11.5 months) showed that proportions and craniometric indices change with age (Stacharski et al., 2010). In this study, a comparison between age groups was not performed, since there were not enough animals in each range to guarantee a reliable characterization. However, it is known that the fusion of the ossification centers occurs between 14 and 20 months of age in the domestic cat, and all animals evaluated were considered adults. To better comprehension of this issue, the authors suggest future research about CFA and CI with a larger sample having different age groups, to state the influence of cranial ossification processes on these indices.

One concern in the present study was the identification of the chiasmatic sulcus for the basic axis and calculate the CFA. It is an anatomical point that is difficult to visualize, even through computed tomography, especially in short skulls, which, if not properly characterized, can influence the measurement of CFA. Thus, as the CFA correlates with the CI, it is possible to calculate the CFA by the equation CI = 103.84-3.30*CFA, provided by the quadratic model, minimizing the chance of error in the investigation of the CFA.

6. CONCLUSION

The reference values of CFA and CI for cats BSH and Persian cats were determined in this study in an unprecedented way, and could be used for the phenotypic classification of cat skulls. Only two cranial types were identified, based on the association of two craniometric parameters, CI and CFA brachycephalic in Persian cats and non-brachycephalic in BSH cats.

7. REFERENCES

BANNASCH, D.; YOUNG, A.; MYERS, J.; TRUVE, K.; et al. Localization of canine brachycephaly using an across breed mapping approach. **PLoS ONE**, v. 5, n. 3, 2010.

CHRISTIANSEN, P.; & HARRIS, J. M. Variation in craniomandibular morphology and sexual dimorphism in pantherines and the sabercat Smilodon fatalis. **PLoS One**, v.7, n.10, p. 1-20, 2012.

EVANS, H. E.; CHRISTENSEN, G. C. **Millers' anatomy of the dog**. Philadelphia: W.B. Saunders Company, 1993.

HAYES, H. M.; PRIESTER, W. A.; & PENDERGRASS, T. W. Occurrence of nervous tissue tumors in cattle, horses, cats and dogs. **International Journal of Cancer**, v. 15, n.1, p. 39–47, 1975.

HENDRICKS, J. Brachycephalic airway syndrome. **Veterinary Clinics of North America-Small Animal Practice**, v. 22, n. 5, p. 1145-1153, 1992.

KOCH, D. A.; WIESTNER, T. B.; MONTAVON, A.; MICHEL, E.; et al. Proposal for a new radiological index to determine skull conformation in the dog. **Schweizer Archiv fur Tierheilkunde**, v. 154, n. 5, p. 217–220, 2012.

KÜNZEL, W.; BREIT, S.; & OPPEL, M. Morphometric investigations of breed-specific features in feline skulls and considerations on their functional implications. **Anatomia Histologia Embryologia**, v. 32, n. 4, p. 218-23, 2003.

LABELLE, A. L.; DRESSER, C. B.; HAMOR, R. E.; ALLENDER, M. C.; et al. Characteristics of, prevalence of, and risk factors for corneal pigmentation (pigmentary keratopathy) in pugs. **Journal of the American Veterinary Medical Association**, v. 243, n. 5, p. 667-674, 2013.

POLLINGER, J. P.; BUSTAMANTE, C. D.; FLEDEL-ALON, A.; SCHMUTZ, S.; et al. Selective sweep mapping of genes with large phenotypic effects. **Genome Research**, v. 15, n. 12, p. 1809–1819, 2005.

REGODÓN, S.; VIVO, J. M.; FRANCO, A.; GUILLÉN, M. T.; et al. Craniofacial angle in dolicho, meso and brachycephalic dogs: radiological determination and application. **Annals of Anatomy**, v. 175, n.4, p. 361-363, 1993.

SABER, A. S.; CACECI, T.; GUMMOW, B.; & JOHNS, K. Morphometric studies on the skull of the Australian domestic cat (*F. catus*) and its clinical implications for regional anesthesia. **Journal of Veterinary Anatomy**, v. 9, n. 1, p. 1-24, 2016.

SCHLUETER, C.; BUDRAS, K. D.; LUDEWIG, E.; MAYRHOFER, E.; et al. Brachycephalic feline noses: CT and anatomical study of the relationship between head conformation and the nasolacrimal drainage system. **Journal of Feline Medicine and Surgery**, v. 11, n. 11, p. 891–900, 2009.

SCHMIDT, M. J.; KAMPSCHULTE, M.; ENDERLEIN, S.; GORGAS, D.; et al. The relationship between brachycephalic head features in modern Persian Cats and dysmorphologies of the skull and internal hydrocephalus. **Journal of Veterinary Internal Medicine**, v. 31, n. 5, p. 1487-1501, 2017.

STACHARSKI, M.; PĘZIŃSKA, K.; WRÓBLEWSKA, M.; WOJTAS, J.; et al. The biometric characteristics of domestic Cat skull in three stages of its growth: **Juvenile, subadult and adult. Acta Scientiarum Polonorum**, v. 9, n. 3, p. 65-78, 2010.

STEFFEN, C.; & HEIDECKE, D. Ontogenetic changes in the skull of the European wildcat (*Felis silvestris*, Schreber, 1777). **Vertebrate Zoology**, v. 62, n. 2, p. 281-294, 2012.

UDDIN, M.; SARKER, M. H. R.; HOSSAIN, M. E.; ISLAM, M. S.; et al. Morphometric investigation of neurocranium in domestic cat (*Felis catus*). **Bangladesh Journal of Veterinary Medicine**, v. 11, n. 1, p. 69-73, 2013.

WEHAUSEN, J. D.; & RAMSEY, R. R. Cranial morphometric and evolutionary relationships in the northern range of *Ovis canadensis*. **Journal of Mammalogy**, v. 81, n. 1, p. 145-161, 2010.

WILLIAMS, D.; MIDDLETON, S.; FATTAHIAN, H.; & MORIDPOUR, R. Comparison of hyaluronic acid-containing topical eye drops with carbomer-based topical ocular gel as a tear replacement in canine keratoconjunctivitis sicca: a prospective study in twenty-five dogs. **Veterinary Research Forum**, v. 3, n. 4, p. 229-232, 2012.

CAPITULO 3

ANATOMICAL DESCRIPTION OF THE NASOLACRIMAL DUCT IN PERSIAN CATS

1. ABSTRACT

This study sought to describe the nasolacrimal duct of Persian cats. Ten cats weighing between 3 and 6 kg (three live cats and seven anatomical samples) underwent bilateral computed tomographic dacryocystography and two skulls were dissected after filling the nasolacrimal duct with latex. Computed tomographic dacryocystography was carried on both sides of each animal, totaling 20 nasolacrimal ducts studied in the horizontal, longitudinal and cross-sectional planes. Length and width of the nasolacrimal duct and lacrimal canaliculi and the shorter distance between the nasolacrimal duct and the root of the upper canine tooth were measured. The nasolacrimal duct followed a tortuous path, particularly in the mid and rostral portions; stenoses (width reduction equal to or greater than 75%) and dilations (width increase equal to or greater than 50%) were also noted, particularly in the rostral portion. Nasolacrimal duct length and width ranged from 1.3 to 1.5 cm and 1.5 to 2.34 mm respectively. Mean lacrimal canaliculus length and width corresponded to 3.1 mm and 0.4 mm respectively. Mean distance from the nasolacrimal duct to the canine tooth was 2.4 mm. The root of the canine tooth interfered with duct trajectory. This study contributed significant anatomical information for clinical assessment of the nasolacrimal drainage system in Persian cats.

KEYWORDS: dacryocystography, nasolacrimal duct, Persian cats, tomography

2. INTRODUCTION

Computed tomographic dacryocystography (CT-DCG) is the contrast-enhanced imaging modality of choice for investigation of nasolacrimal duct anatomy and diagnosis of pathological conditions such as obstructions, stenoses, fistulae, diverticula and incomplete duct filling caused by calculi or tumours (Kanski, 2004a, 2004b). This imaging modality has been used in studies describing normal nasolacrimal duct anatomy and cross-sectional area in bone specimens (Shokry et al., 1987; Spiess & Pot et al., 2013) and investigating nasolacrimal duct abnormalities in humans (Freitag et al., 2002; Yong et al., 2014; Kumar et al., 2016), dogs (Eisner, 1996; Benigni & Lamb, 2006; Nöller et al., 2006), buffaloes (Bigham & Shadkhast, 2009), llamas (Sapienza et al., 1992), cats (Anthony et al., 2010; Paiva et al., 2013), dromedaries (Shokry et al., 1987), rabbits (Hou et al., 2017), horses (Adams et al., 2013) and cattle (Braun et al., 2014; Jugant et al., 2019).

Direct computed tomographic measurement is a reliable method for investigation of gender- and age-related nasolacrimal duct width differences (Takahashi et al., 2011) and may also be used for anatomical assessment prior to clinical examination or surgical planning. This study set out to describe the nasolacrimal drainage system of Persian cats using CT-DCG and skull dissection.

3. MATERIALS AND METHODS

3.1. Animals

Ten Persian cats (three alive cats and seven anatomical specimens) weighing between 3 and 6 kg were used in this study (Table 1). Alive cats were recruited from routine clinical practice at veterinary hospitals. Cats dead of natural causes unrelated to this study and obtained from different sources were used for anatomical specimen preparation. All cats in this study had normal lacrimal puncta. Alive cats were also free from ocular or otological abnormalities. The sample was classified according to degree of brachycephaly, as by Schlueter et al., (2009).

Table 1. Age, gender and body weight of cats included in the sample, and nasolacrimal duct assessment method

ANIMAL	GENDER	AGE (YEARS)	WEIGHT (KG)	METHOD
1	M	5	5.4	CT-DCG
2	M	10	5.2	CT-DCG
3	F	8	4.6	CT-DCG
4	M	4	3.7	CT-DCG
5	F	8	6.6	CT-DCG
6	M	2	4.1	CT-DCG
7	M	8	5.2	CT-DCG
8	M	7	5.3	CT-DCG
9	M	10	5.4	CT-DCG + LATEX
10	F	9	4.9	CT-DCG + LATEX

CT-DCG: Computed tomographic dacryocystography

3.2. Computed tomographic dacryocystography (CT-DCG)

Cats in this study were submitted to bilateral computed tomographic dacryocystography (CT-DCG). Alive cats received preanesthetic medication consisting of intramuscular administration of acepromazine and morphine (Acepran®, Univet and Dimorf®, Cristália; 0.05 mg/kg and 0.5mg/kg respectively). Dissociative anesthesia was then induced with intravenous tiletamine/zolazepam (Zoletil 50®, Virbac; 5 mg/kg) administration. None of the corpses were frozen before dacryocystography. The cats were placed in sternal decubitus and post-contrast images obtained in the transverse (axial), sagittal (longitudinal) and coronal (horizontal) planes using a single detector helical computed tomography (HiSpeed LX / i - General Electric Company, Medical Systems, USA) and the following configurations: rotation time of 1.0 s, tension of 120 kV, voltage of 150 mA and slice thickness 1.0 mm. The cadaveric samples were scanned using the same protocol.

All 20 lower lacrimal punctum were cannulated using a 24 G x 0.75 ”intravenous catheter (Angiocath Jelco® 24G; Becton Dickinson, BD). Tomographic images were then acquired in the non-contrast phase, for appropriate collimation selection. The upper lacrimal puncture was digitally occluded to prevent reflux of the contrast agent and 0.5 mL of water-

soluble iodinated contrast material (Ioexol, Omnipaque ® 300mg / dL; GE Healthcare) injected in one time, through the catheter, using a 100 IU insulin syringe (Becton Dickinson, BD), escaping through the nasolacrimal ostium or into the oral cavity was observed. Contrast images were acquired immediately after injection of the contrast agent, without removing the catheter. The three-dimensional reconstruction of the image was performed using built-in software (bone algorithm; window level from 200 to 2250 UH and bone filter for noise reduction). The images were stored in the standard DICOM format.

The nasolacrimal duct was described in its entire length, from the lacrimal sac to the nasolacrimal duct opening into the nasal cavity. Measurements were made using Radiant Dicom software. The distance between the root of the upper canine tooth and the rostral portion of the nasolacrimal duct was measured in both antimeres (M1R and M2L, rigth and left respectively) and the shorter length determined (Fig. 1D). These measurements were made in the cross-sectional plane, at the level of the upper canine tooth alveolus. Right and left nasolacrimal duct length (LDR and LDL respectively) were measured in the sagittal plane. Length (CLR; CLL) and maximum width (CDR; CDL) of the right and left lacrimal canaliculi were also measured in the cross-sectional plane, at the level of the infraorbital canal (Fig. 1A and 4D). Right and left nasolacrimal duct width were measured in the cross-sectional plane at two sites: (D1) at the level of the second upper premolar tooth, where the nasolacrimal duct enters the nasal cavity, beyond the maxillary bone (Fig. 1B); and (D2) at the level of the upper canine tooth, where the nasolacrimal duct opens into the nasal vestibulum, just dorsal the hard palate (Fig. 1C). Nasolacrimal duct stenosis (width reduction equal to or greater than 75%) and dilation (width increase equal to or greater than 50%) were also investigated.

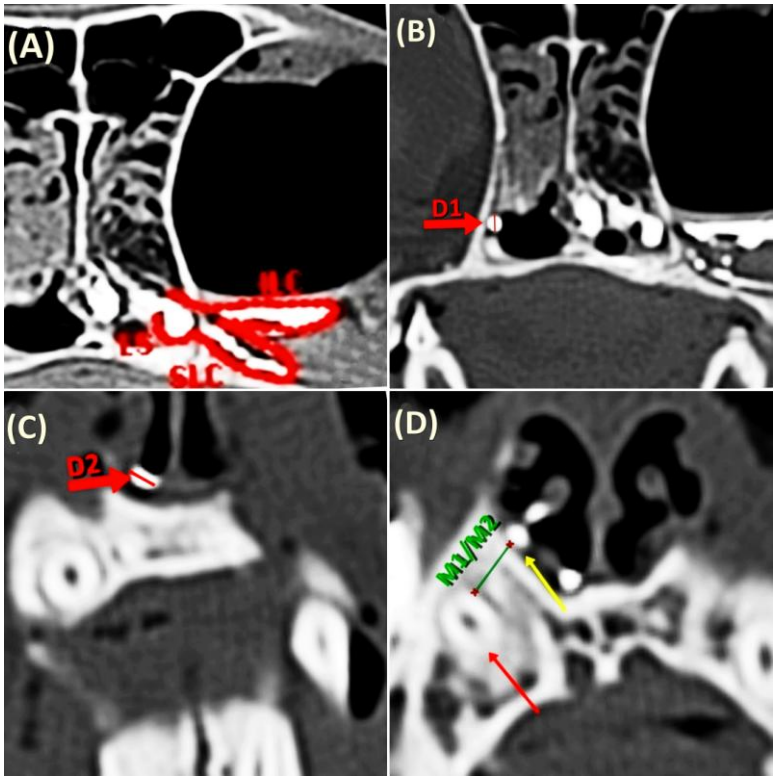

Figure 1. Contrast-enhanced CT. **A** – Cross-sectional image acquired at the level of the infraorbital canal. **(ILC)** Lower lacrimal canaliculus; **(SLC)** Upper lacrimal canaliculus; **(LS)** Lacrimal sac. **B** - Cross-sectional image acquired at the level of the 2nd premolar. **(D1)** Duct width measurement site. **C** - Cross-sectional image acquired at the level of the upper canine tooth. **(D2)** Duct width measurement site within the nasal vestibulum. D - Cross-sectional image acquired at the level of the upper canine tooth. **(E) M1** and **(D) M2** measurement. **Yellow arrow**: nasolacrimal duct. **Red arrow**: root of the upper canine tooth.

3.3. Latex

Both nasolacrimal ducts of two cadaveric specimens were injected with blue latex immediately after CT-DCG via the same catheter used for contrast material injection. Specimens were then fixed in 10% formaldehyde solution and used for skull dissection and exposure of the nasolacrimal duct.

3.4. Gross nasolacrimal duct anatomy

Cadaveric specimens were dissected and photographed. Dissection started with mid-sagittal section of the skull using a powered band saw, from the rostral end of the nare to the caudal end of the squamous, and basilar portions of the occipital bone. Left and right external eye structures were identified, the skin reflected laterally and orbital exenteration performed. Nasal conchae were gradually and carefully then removed, starting at the level of the nasal

septum. Finally, the maxillary and lacrimal bones surrounding the nasolacrimal duct were filed away using a rotating micro drill to expose the latex-filled duct.

This study was approved by the Ethics Committee for Animal Use of University of Brasília (CEUA/UnB), protocol No. 66690/2016. Anatomical descriptions were rendered according to *Nomina Anatomica Veterinaria – NAV* (2017) and related publications.

4. STATISTICAL ANALYSIS

Descriptive analysis was conducted to describe variables behavior. Then, an analysis of variance was performed using a the weight variable, according to a completely randomized design (DIC), in which the factor studied was only sex. For the other variables, an analysis of variance was also performed according to a DIC in a factorial arrangement 2 (sex) x 2 (antimere). Finally, a correlation analysis between all variables was performed for each anomer.

The descriptive, variance and correlation analyzes of the data were conducted respectively using the MEANS, MIXED and CORR procedures of the Statistical Analysis System software (SAS; version 9.2). To consider a significant effect, a probability level of 5% or less for the tests used was adopted.

5. RESULTS

The lacrimal film drainage apparatus consisted of lacrimal puncta, lacrimal canaliculi, lacrimal sac and nasolacrimal duct. Upper and lower lacrimal puncta were identified in all samples. These were located within the conjunctival sac, at the medial angle of the eye, close to the medial palpebral commissure. Lower lacrimal punctum cannulation was achieved in all cases. The upper and lower lacrimal puncta corresponded to the openings of the lacrimal canaliculi. These were fused ventrally to the medial angle of the eye and opened directly into the lacrimal sac located within the lacrimal sac fossa of the lacrimal bone.

The nasolacrimal duct originated in this sac and appeared as a cone-shaped dilation within the lacrimal sac fossa of the lacrimal bone (Fig. 1A). Computed tomographic DCG yielded cross-sectional, horizontal and longitudinal images. The prominent frontal process of the lacrimal bone, the lacrimal sac fossa and the ventral nasal concha marked the starting point of the nasolacrimal duct (Fig. 2A-D). Skull conformation was consistent with grade 2 brachycephaly (Schueleter et al., 2009) in all cases, i.e., incipient dorsorotation of the upper canine teeth and jaw, shortened nasal bone and rounded or apple-shaped neurocranium (Fig. 2C).

Total duct length ranged from 1.3 to 1.7 cm. Canaliculi followed a straight path and joined each other at the lacrimal sac. Upper and lower lacrimal canaliculi could be identified in both antimeres and had similar length and width (3.1 and 0.4 mm on average). The root of the canine tooth was contained within the alveolar tissue of the maxillary bone, approximately 2,39 mm ventrolateral to the nasolacrimal duct (Table 2; Fig. 1D).

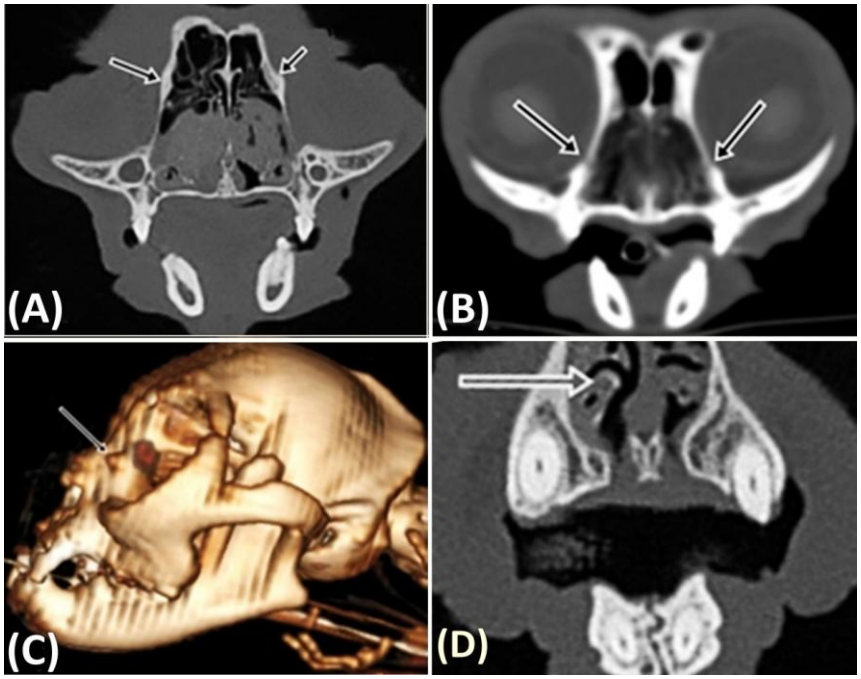

Figure 2. A – Cross-sectional image acquired at the level of the infraorbital foramen. Note the frontal process of the lacrimal bone (arrows). **B** - Cross-sectional image acquired at the level of the maxillary foramen. Note the lacrimal sac fossa (arrows). **C** – 3D reconstruction. Note the frontal process of the lacrimal bone (arrow). **D** - Cross-sectional image acquired at the level of the fenestra of the ventral concha. Note dorsal displacement of the ventral nasal concha (arrow).

Table 2. Descriptive analysis of study variables (body weight, distance between the nasolacrimal duct and the root of the upper canine tooth, and width and length of nasolacrimal duct and lacrimal canaliculi)

Variable	Sex	Antimere	N	Mean	SD	CV (%)	Min	Max
Body weigth (kg)	Both	-	10	5.04	0.796	15.8	3.70	6.60
LD (cm)	Both	Both	20	1.47	0.124	8.5	1.31	1.73
CL (mm)	Both	Both	20	3.15	0.193	6.1	2.80	3.50
CD (mm)	Both	Both	20	0.40	0.022	5.5	0.37	0.45
D1 (mm)	Both	Both	20	2.34	0.255	10.9	1.98	2.78
D2 (mm)	Both	Both	20	1.48	0.234	15.7	1.12	1.90
M (mm)	Both	Both	20	2.39	0.282	11.8	1.81	2.87

N: number of observations; **SD:** standard deviation; **CV:** coefficient of variation; **Min:** minimum; **Max:** maximum; **LD (right and left):** duct lacrimal length; **CL (right and left):** canaliculus lacrimal length; **CD (right and left):** canaliculus lacrimal diameter; **D1:** nasolacrimal duct width at the at the level of the second upper premolar tooth; **D2**: nasolacrimal duct width at the level of the upper canine tooth; **M** (M1L and M2R)**:** Distance from nasolacrimal duct to root of upper canine tooth.

Dorsal displacement of the ventral nasal concha was confirmed in all cats in this study (Fig. 3C, 3D). Computed tomographic dacryocystography revealed nasolacrimal duct patency in all cats, confirmed by the presence contrast material at the distal end of the nasolacrimal ostium. Contrast agent volume (0.5 mL) was therefore enough to fill the lacrimal drainage apparatus in all specimens. The nasolacrimal duct coursed rostrally at the medial aspect of the maxillary bone (mid portion of the nasolacrimal duct), then ran ventrally to the basal fold of

the ventral concha, where it was displaced by the apex of the upper canine tooth root and exited the nasal cavity (Fig. 4A). Finally, the duct penetrated the ventrolateral aspect of the nasal vestibulum to reach the nasolacrimal ostium, below the basal fold of the ventral concha (rostral portion of the nasolacrimal duct) (Fig. 4C and 7B). This portion of the duct was covered exclusively by mucous membrane.

The width of the nasolacrimal duct between the antimers, both in D1 and D2) did not differ significantly between cats (Table 3). However, males showed statistically higher D1 and D2 values compared to females (Table 3). Both the length and the diameters of the nasocrimal duct were statistically greater in the male cats studied. The average distances left and right between the nasolacrimal duct and the root of the upper canine (M1R and M2L) did not differ significantly, but it was higher in females (Table 3). The correlation analysis (Pearson's correlation coefficient) showed a strong positive correlation ($P < 0.05$), body weight, length and width of the tear ducts. In addition, a positive correlation was demonstrated between the length of the nasolacrimal duct and the diameters measured in D1 and D2 (Table 4).

Table 3. Effect of gender on study variables (body weight, distance between the nasolacrimal duct and the root of the upper canine tooth, and width and length of nasolacrimal duct and lacrimal canaliculi)

Variable	Sex (S)		Antimere (A)		*P*-value		
	Female	Male	Right	Left	S	A	S × A
BW (kg)	5.03 (0.488)	5.04 (0.319)	-	-	0.9874	-	-
LD (cm)	1.35 (0.023)^{b}	1.52 (0.031)^{a}	1.44 (0.026)	1.43 (0.029)	0.0006	0.8794	0.9468
CL (mm)	3.17 (0.090)	3.14 (0.055)	3. 15 (0.075)	3.15 (0.074)	0.7773	0.9478	0.9478
CD (mm)	0.39 (0.008)	0.40 (0.006)	0.39 (0.004)	0.40 (0.009)	0.4210	0.3546	0.7714
D1 (mm)	2.08 (0.038)^{b}	2.45 (0.062)^{a}	2.27 (0.051)	2.27 (0.051)	0.0001	1.0000	1.0000
D2 (mm)	1.31 (0.029)^{b}	1.56 (0.068)^{a}	1.43 (0.052)	1.43 (0.052)	0.0048	1.0000	1.0000
M (mm)	2.54 (0.034)^{a}	2.32 (0.087)^{b}	2.43 (0.066)	2.43 (0.066)	0.0348	0.9283	0.6862

Least squares means (standard error); **BW:** body weight; **LD (right and left):** duct lacrimal length; **CL (right and left):** canaliculus lacrimal length; **CD (right and left):** canaliculus lacrimal diameter; **D1:** nasolacrimal duct width at the at the level of the second upper premolar tooth; **D2**: nasolacrimal duct width at the level of the upper canine tooth; **M** (M1L and M2R)**:** Distance from nasolacrimal duct to root of upper canine tooth. ^{a,b}Means followed by different letters between the sexes differ at a significance level of 5% by the test *F*.

Table 4. Pearson's correlations for variables (body weight, distance between the nasolacrimal duct and the root of the upper canine tooth, and width and length of nasolacrimal duct and lacrimal canaliculi) in Persian cats

Variable	LD	CL	CD	D1	D2	M
Right antimere						
BW	0.56	**0.85**	**0.65**	0.56	0.55	0.27
LD		0.45	**0.69**	**0.78**	**0.79**	–0.42
CL			0.61	0.28	0.55	0.25
CD				0.50	**0.65**	0.09
D1					0.58	–0.05
D2						–0.09
Left antimere						
BW	0.57	0.03	–0.41	0.56	0.55	**0.67**
LD		0.28	0.00	**0.79**	**0.77**	0.07
CL			–0.02	-0.08	0.06	–0.02
CD				-0.38	0.05	–0.43
D1					0.58	0.24
D2						0.26

BW: body weight; **LD (right and left):** duct lacrimal length; **CL (right and left):** canaliculus lacrimal length; **CD (right and left):** canaliculus lacrimal diameter; **D1:** nasolacrimal duct width at the at the level of the second upper premolar tooth; **D2**: nasolacrimal duct width at the level of the upper canine tooth; **M** (M1L and M2R)**:** Distance from nasolacrimal duct to root of upper canine tooth. Correlation coefficients in bold are statistically different from zero (P<0.05).

The nasolacrimal duct then followed a short course through the lacrimal bone, crossed the lacrimal canal of the maxillary bone (caudal one-third of the nasolacrimal duct) and continued rostrally and parallel to the hard palate, inside the nasal cavity (Fig. 4A and 4D). This duct segment remained attached to the nasal mucosa up to the level of the basal lamina of the ventral nasal concha. At the mid portion of the nasal cavity, the nasolacrimal duct was displaced by the ventral concha at a 90° angle (Fig. 4D and 7B).

Tomographic artifacts resulting from contrast agent escape were noted in seven (7) cats, at the following sites: distal lacrimal puncta, nasal commissure, nasal cavity and external extremity of the nares, over the incisor bone (Fig. 4D and 5A). Contrast material was also detected in the left and right tympanic cavities in two (2) cats (Fig. 5B and 5C). Nasolacrimal ducts in this sample had no accessory openings.

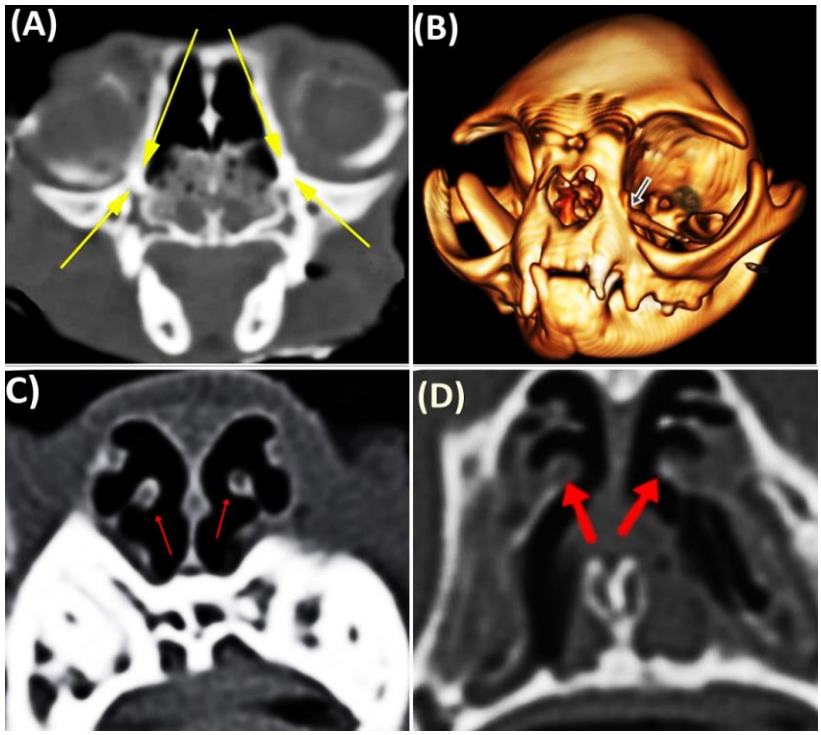

Figure 3. A – Cross-sectional image acquired at the level of the infraorbital foramen. Note the opening of the nasolacrimal duct into the nasal cavity. **B** - 3D reconstruction. Note the site of entry of the nasolacrimal duct into the lacrimal bone, at the level of the 2nd upper premolar tooth, **C** - Cross-sectional image acquired at the level of the upper canine tooth. Note alar folds (red arrows) along the dorsally displaced ventral nasal concha (**red arrows, D**).

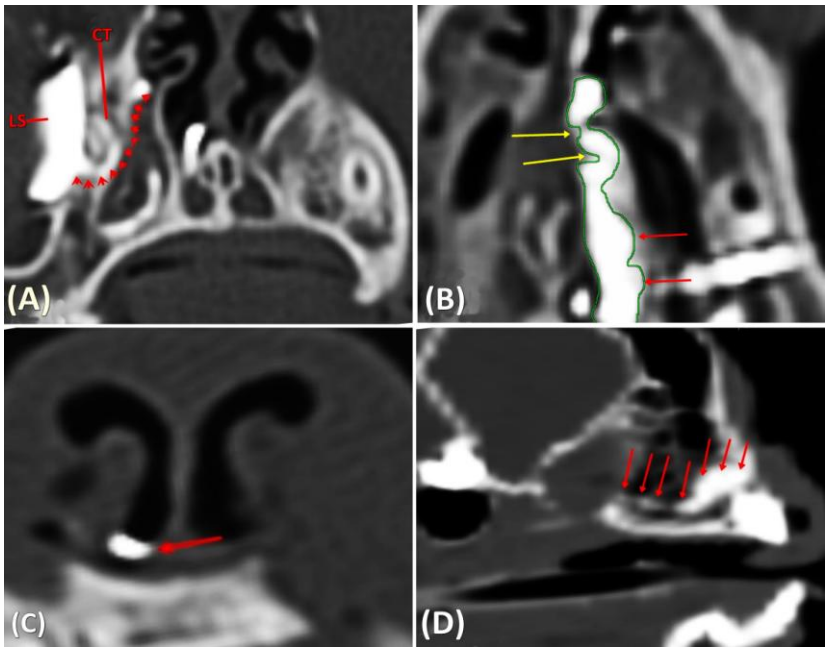

Figure 4: Contrast-enhanced CT. **A** – Cross-sectional image acquired at the level of the infraorbital canal. **(LS)** lacrimal sac; (CT) root of the upper canine tooth and nasolacrimal duct trajectory (red arrows). Note bend in nasolacrimal duct for efficient lacrimal sac drainage. **B** - Cross-sectional image acquired at the level of the ventral nasal meatus. Note nasolacrimal duct tortuosity, dilatations (red arrows) and stenoses (yellow arrows). **C** - Cross-sectional image acquired at the level of the incisor bone. Note the nasal ostium of the nasolacrimal duct on the ventrolateral aspect of nasal vestibulum. **D** - Sagital-sectional image acquired at the level of the hard palate. Note nasolacrimal duct trajectory (red arrows) and displacement dorsal to the root of the canine tooth.

Tortuous duct trajectory, visible as irregular contrast-agent columns within the mid and rostral portions of the nasolacrimal duct, between the basal lamina of the ventral nasal concha and the site of entry into the nasal vestibulum (Fig. 4B, 5A, 6A and 6C), was confirmed in all cats in this sample. Ductal stenosis appearing as narrowed contrast-agent columns in the mid portion of the duct, rostromedially to the canine tooth (Fig. 6A-D) was also detected in all cases. Tomographic images in this study revealed mid portion and rostral nasolacrimal duct dilations (Fig. 4B, 5A, 6A and 6B) in all cats.

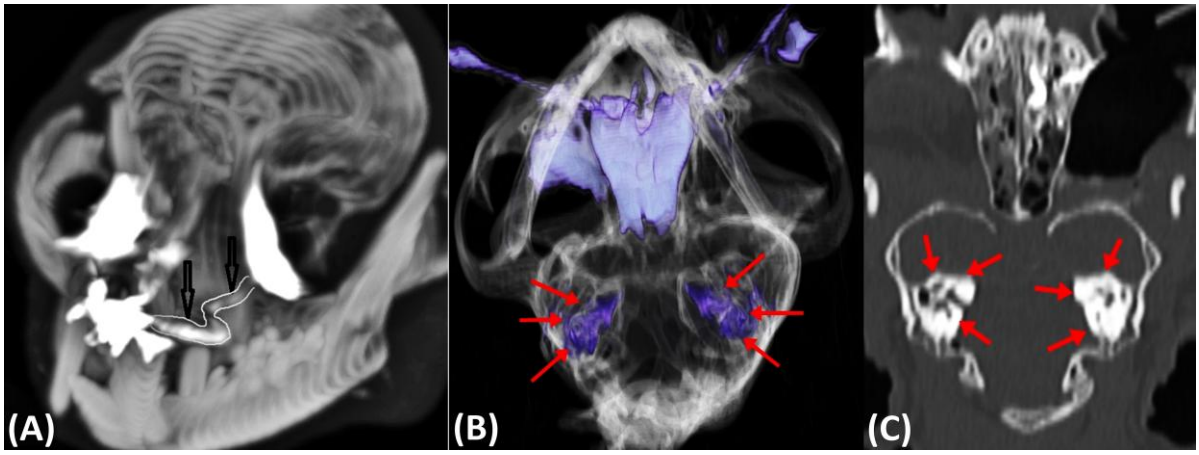

Figure 5: 3D reconstructions. **A** – Persian cat skull. Note nasolacrimal duct tortuosity (arrows). **B** – Computed tomographic dacryocystography; cross-sectional image acquired at the level of the upper canine tooth. Note contrast material in the tympanic cavities (**C** - arrows)

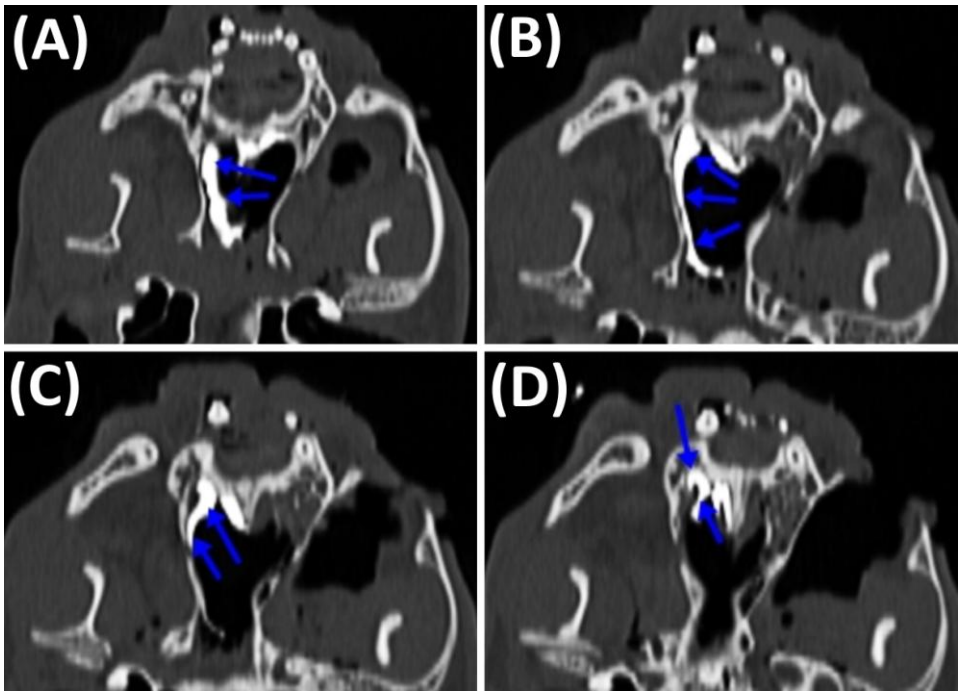

Figure 6: Contrast-enhanced CT. **A-D** – Horizontal images. The nasolacrimal duct is depicted in its entire length. Note duct tortuosity, dilatations and stenoses.

The lacrimal bone was located rostrally to the infraorbital foramen (Fig. 7A), at the level of the distal aspect of the second upper premolar tooth. Approximately 25% of this length was contained within the lacrimal canal formed by the lacrimal and maxillary bones. The wide and tortuous duct comprised caudal, mid and rostral portions. The caudal portion lied within a ventrally convex, bow-shaped bony canal formed by the lacrimal and maxillary bones. The mid portion was located at the medial wall of the maxillary bone, underneath the nasal mucosa. Finally, the rostral portion comprised the free portion of the duct, which opened into the nasolacrimal ostium located at the junction of the medial and lateral walls of the nasal vestibulum, approximately 0.4 cm from the external nare (Fig. 7B and 7C).

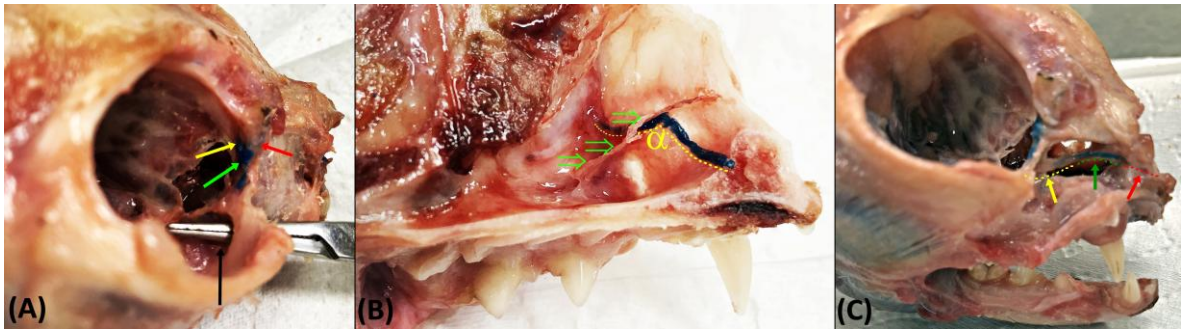

Figure 7. **A** - Photomacrograph of the Persian cat skull. Note lacrimal canaliculi (yellow and red arrows), lacrimal sac (green arrow) and infraorbital foramen (black arrow). **B** - Left midsection of a Persian cat skull following blue stained latex injection and removal of nasal septae and conchae. α: angle formed by the draining trajectory of the nasolacrimal duct due to displacement by the conchal crest. Note the basal lamina of the ventral nasal concha (green arrows) **C**: Photomacrograph of a Persian cat skull; the nasolacrimal duct is filled with pigmented latex. Note nasolacrimal duct caudal, mid and cranial segments (yellow, green and red arrows respectively), ventral convexity of the caudal segment and dorsal convexity of the cranial segment.

Methods used to investigate nasolacrimal duct anatomy in this study were deemed complementary and yielded similar findings. Biometric measurements were limited to CT-DCG. This method also allowed better appreciation of duct stenosis and tortuous trajectory compared to dissection. Cadaveric specimen dissection confirmed 3D tomographic reconstruction findings, particularly the dorsal displacement of the ventral nasal concha and the impact of shortened facial bones on nasolacrimal duct trajectory.

6. DISCUSSION

Contrast-enhanced tomographic assessment and gross dissection were deemed appropriate for location and anatomical description of structures forming the tear drainage system of Persian cats. Despite narrow width and superimposition on the lacrimal and maxillary bones, nasal conchae and nasal septum, patency of lacrimal drainage system structures could be confirmed, as reported elsewhere (Nykamp et al, 2004). As in most domestic species, approximately ¼ of the nasolacrimal duct of Persian cats was contained within a bony scaffold in the nasal cavity. These anatomical features may limit the value of CT-DCG for detection of subtle (less than 75% width reduction) duct stenosis. Such subtle stenoses were not investigated in this study; therefore, no biases were introduced in the analysis Sapienza et al., 1992; Yoshikawa et al., 2000, Spiess & Pot et al., 2013).

Similar to CT-DCG techniques used in humans (Nykamp et al., 2004; Rached et al.,2011), cross-sectional plane CT yielded better images for assessment of duct trajectory, whereas combined horizontal and longitudinal plane imaging allowed overall duct assessment and detection of stenoses and tortuosities (Fig. 4D; 6A-D). This reflects spatial relationships between the nasolacrimal duct and the skull in cats. Different from the prevailing dorsoventral orientation of the nasolacrimal duct in humans, the nasolacrimal duct of cats runs in a rostrocaudal direction and is more accurately depicted in cross-sectional tomographic images. Cross-sectional images are particularly useful for biometric measurements and investigation of interactions between skull bones and the nasolacrimal duct.

Tomographic slice thickness selection was a major concern in this study, given the small size of lacrimal drainage system structures. The risk of missing imaging data is greater in 2 mm compared to 0.8 mm axial slices. Slice thickness of 1 mm was therefore adopted in this study, as excessively thin slices may increase image noise and decrease spatial resolution (Freitag et al., 2002; Rached et al., 2011).

The prominent frontal process of the lacrimal bone (Fig. 2A) observed in cats in this study was thought to be a unique anatomical feature and served as a landmark for nasolacrimal duct location in tomographic images. Dorsal displacement of the ventral nasal concha interfering with nasolacrimal duct trajectory in brachycephalic cats (Breit et al., 2003; Schuleter et al., 2009) has been confirmed in this sample and may impair lacrimal drainage in these animals.

Different from other studies (Breit et al., 2003; Schuleter et al., 2009), iodinated contrast agent recommended for contrast-enhanced tomography did not remain in the nasolacrimal duct of cats in this sample during CT-DCG. This may have reflected low contrast agent viscosity and rapid passage through the duct, making duct delineation difficult. Continuous contrast agent injection immediately prior to tomographic assessment was required given the narrow width of the target structure. Cats also had to be restrained in sternal recumbence for appropriate nasolacrimal duct filling (Breit et al., 2003; Habbin, 1993). Alternative contrast agents such fat soluble products or microbubbles may offset technical constraints associated with rapid outflow in CT-DCG. Patient position and contrast agent characteristics should be accounted for in tomographic imaging technique selection (Takehara et al., 2000).

As it is a fundamentally anatomical tomographic study, we decided to use only two animals for dissecting the duct, complementing the tomographic findings. Anatomical data obtained via dissection played a significant role in tomographic image interpretation. Missing lacrimal puncta and micropuncta, functional stenosis and fibrosis have been reported in Persian cats (Stades et al., 1999; Dyce et al., 2010; Anthony et al., 2010). However, patent lower and upper lacrimal puncta, with no signs of functional stenosis or fibrosis, were identified in all cats in this sample. As reported in Persian (Schlueter et al., 2009) and European cats (Nöller et al., 2006) the nasolacrimal duct originated at the level of the second premolar tooth in specimens in this study. Similar anatomical findings in unrelated cats of different origins in this sample emphasize breed-specific characteristics.

The biometric analysis of the structures that make up the lacrimal drainage apparatus allowed comparisons with other breeds and species of cats. The shorter nasolacrimal duct in cats in this sample, compared to domestic shorthaired cats in another study (1.3 to 1.7 cm and 2.5 to 4 cm, respectively) is consistent with the short and round skull of Persian cats (Gelatt et al., 1992). Greater nasolacrimal duct width (1.1 mm to 2.7 mm; Table 2) compared to previous width measurements in brachycephalic dogs and cats (Gelatt et al., 1992; Nykamp et al., 2004; Gelatt, 2003) suggest that Persian cats have a wider duct compared to other animals

with a similar skull shape. This fact suggests that the higher prevalence of epiphora in the Persians is not related only to the diameter of the nasolacrimal duct.

Close topographic relationships between the nasolacrimal and the root of the upper canine tooth (mean distance 2.39 mm) may be a predisposing factor for duct obstruction in response to apical maxillary canine periodontitis, calculosis or crown fratures (Ramsey et al., 1996; Augsburger et al., 2012). Iatrogenic complications inherent to tooth extraction in this anatomical region may also lead to extramural nasolacrimal duct obstruction (Ramsey et al., 1996; Eisner, 1996; Schlueter et al., 2009; Anthony et al., 2010).

Efficient lacrimal drainage is thought to be a function of nasolacrimal duct trajectory and width (Michel, 1955; Breit et al., 2003; Schlueter et al., 2009). However, as the duct diameter found here was larger compared to other brachycephalics, it is suggested that the epiphora is unrelated with the diameter of the duct.

Findings of this study support reported correlations between nasolacrimal duct width and body weight in Persian cats (Rached et al., 2011. Nasolacrimal duct width varied according to site of measurement (D1 or D2), as described by Rached et al. (2011). The nasolacrimal duct was narrower in the rostral compared to the mid portion. Significant differences in duct width measured at the level of the second upper premolar tooth (D1) between male and female cats in this sample may have reflected sexual dimorphism or represented an incidental finding (Park et al., 2016).

Duct dilations were detected primarily at the mid portion and may be associated with shortened facial bones and dorsal displacement of the nasal concha. However, anastomoses between a dense vascular plexus and the nasolacrimal duct in this region of the nasal cavity have been described in humans. Even though this vacularization is adjacent to the duct, it can have dynamic physiological implications for duct function due to duct dilation or contraction in response to autonomous stimuli, which in turn can contribute to the prevalence of epiphora. Studies comparing brachycephalic and non-brachycephalic cats are warranted for detailed investigation of nasal cavity vascularization (Thale et al., 1998; Schlueter et al., 2009).

Cats in this study had dilated, well-developed lacrimal sacs. Similar findings have been described in mesaticephalic and brachycephalic dogs, but had not been reported in Persian cats to date. These anatomical features may be associated with lower prevalence of lacrimal sac obstruction secondary to retained foreign bodies or inflammatory reactions in brachycephalic cats. The accumulation of tears in response to the marked dilation of the lacrimal sac may explain high rates of negative responses in tests designed to assess the

patency of the nasolacrimal duct in brachycephalic cats, such as the Jones test (Gelatt et al., 1995; Spiess & Pot et al., 2013).

As previously reported (Breit et al., 2003; Nöller et al., 2006), the nasolacrimal duct is in direct contact with the nasal cavity mucosa, with no bony protection. Close anatomical relationships between these structures and potential extramural lacrimal sac compression support cause-effect relationships between lacrimal sac inflammation and pathological conditions affecting the nasal or oral cavity, such as ectopic teeth and nasal tumors and cysts (Nöller et al., 2006, Stiles & Townsend, 2007; Spiess & Pot, 2013; Voelter-Ratson et al., 2014).

Abnormal nasolacrimal system drainage into the caudal aspect of the nasal cavity/nasopharynx or the oral cavity has been reported in brachycephalic dogs and may apply to brachycephalic cats (Kern, 1986; Michel, 1995; Gelatt, 2001; Grahn & Sandmeyer, 2007; Ollivier, 2007). However, in a study with 36 non-brachycephalic cats the nasolacrimal duct drained into the ventrolateral aspect of the nasal vestibulum floor, below the alar fold, and no anomalous openings were found (Binder & Herring, 2010). Likewise, cats in this sample had no accessory or anomalous duct openings. Future studies with larger samples and comparing brachycephalic and non-brachycephalic cats are warranted to fill this gap in anatomical knowledge.

The relationship between nasolacrimal duct trajectory and skull shape in brachycephalic cats in this sample revealed a rostrodorsal portion of the duct running parallel to the hard palate and reaching the apex of the upper canine tooth alveolus. Maxillary dorsorotation and facial shortening caused by caudal displacement of the upper canine tooth root in these cats affect nasolacrimal duct orientation and may impair tear drainage, leading to epiphora (Schlueter et al., 2009).

Contrast material extravasation into the tympanic cavities in the absence of otitis media occurred in two cats in this sample and is a common finding in brachycephalic humans with nasopharyngeal stenosis (Worley et al., 1994). Contrast agent may escape into the nasal cavity during CT-DGT, spread to the nasopharynx, enter the auditory tube and reach the rostral portion of the tympanic cavities (Nykamp et al., 2004; Njaa et al., 2012; Casselbrant et al., 2013).

Establishment of reference ranges for nasolacrimal duct width at different sites in brachycephalic and non-brachycephalic cats belonging to different body weight categories may support comparative anatomy studies and help elucidate controversial relationships between duct width and epiphora, a common occurrence in these animals.

The interpretation of the tomographic image was a great challenge in this study, due to the small dimensions of the duct and the overlapping of structures. Specific training requirements and time-consuming nature of the evaluation of the nasolacrimal duct image-based CT were emphasized during this study and also elsewhere. (Czyz et al., 2015).

Given the wide variation in skull shape and degree of brachycephaly in Persian cats, small sample size may have been a limiting factor in this study. This sample failed to contemplate all degrees of facial shortening (Schlueter et al., 2009). However, it was fairly homogeneous with respect to degree of brachycephaly (grade II).

Technical challenges in this study (rapid contrast agent flow through the nasolacrimal duct in particular) must be emphasized. Still, difficulties in CT-DCG protocol standardization were not thought to have impacted final image quality.

7. CONCLUSION

Gross dissection and CT-DCG revealed a wider and more tortuous nasolacrimal duct in Persian cats compared to brachycephalic dogs. Lacrimal sac dilations and higher numbers of stenotic sites were also detected. These anatomical features may be related to chronic epiphora and negative Jones test responses in this species. Finally, the prevalence of accessory nasolacrimal duct openings in Persian cats should be questioned.

8. REFERENCES

ADAMS, M. F.; CASTRO, J. R.; MORANDI, F.; REESE, R. E, AND REED, R. B. The nasolacrimal duct of the mule: Anatomy and clinical considerations. **Equine veterinary education**, v. 25 n. 12, p. 636-642, 2013.

ANTHONY, J. M. G.; SANDMEYER, L. S.; LAYCOCK, A. R. Nasolacrimal obstruction caused by root abscess of the upper canine in a cat. **Veterinary Ophthalmology**, v. 13, n. 2, p. 106–109, 2010.

AUGSBURGER, A.-S.; DECOUVELAERE, E. & HERICHER, T. Un cas d'occlusion lacrymale chez un chat : conséquence d'une nécrose dentaire sur l'évacuation lacrymale. **Pratique Médicale et Chirurgicale de l'Animal de Compagnie**, v. 47, n. 2, p. 37–42, 2012.

BENIGNI, L.; LAMB C. Diagnostic imaging of ear disease in the dog and cat. **In Practice**, v. 28, p. 122-130, 2006.

BIGHAM, S. A., SHADKHAST, M. Apparatus of Iranian River Buffaloes (Bubalus bubalis): Anatomical Study. **Vet Scan**, v. 4, 2009.

BINDER, D. R.; & HERRING, I. P. Evaluation of nasolacrimal fluorescein transit time in ophthalmically normal dogs and non brachycephalic cats. **American Journal of Veterinary Research,** v. 71, n. 5, p. 570–574, 2010.

BRAUN, U.; JACOBER, S. AND DRÖGEMÜLLER, C. Congenital nasolacrimal duct fistula in Brown Swiss cattle. **BMC Veterinary Research**, v. 10, n. 1, p. 44, 2014.

BREIT, S.; KÜNZEL, W.; OPPEL, M. The course of the nasolacrimal duct in brachycephalic cats. **Anatomia Histologia Embryologia,** v. 32, n. 4, p. 224–227, 2003.

CASSELBRANT, L. M.; SWARTS, J. D.; MANDEL, E. M.; DOYLE, W. J. The Cephalic Index is not different among groups of children aged 36–48 months with chronic otitis media with effusion, recurrent acute otitis media and controls. **International Journal of Pediatric Otorhinolaryngology,** v. 77, n. 3, p. 334–337, 2013.

CZYZ, C. N.; BACON, T. S.; STACEY, A. W.; CAHILL, E. N.; COSTIN, B. R.; KARANFILOV, B. I.; CAHILL, K.V. Nasolacrimal system aeration on computed tomographic imaging: effects of patient positioning and scan orientation. **Clinical Ophthalmology**, v. 9, p. 469-473, 2015.

DYCE, K. M.; SACK, W. O. & WENSING, C. J. G. **The locomotor apparatus, the nervous system, the head and ventral neck of the dog and cat**. In: Dyce, K. M., Sack, W.O., Wensing, C. J. G. 4ª edition. Saint Louis, Missouri: Elsevier Health Sciences, 2010.

EISNER, E. R. Nonsurgical and surgical tooth extraction and oronasal fistula repair. **Canine Practice**, v. 21, p. 12–15, 1996.

FREITAG, S. K.; WOOG, J. J.; KOUSOUBRIS, P. D.; CURTIN, H. Helical computed tomographic dacryocystography with three-dimensional reconstruction: a new view of the lacrimal drainage system. **Ophthalmic Plastic and Reconstruction Surgery**, v. 18, n. 2, p. 121–132, 2002.

GELATT, K. N. **Surgery of the nasolacrimal apparatus and tear systems**. In: Gelatt KN, ed. Small animal ophthalmic surgery. Woburn, Mass: Butterworth-Heinemann, 125–141, 2001.

GELATT, K. N. **Doenças e cirurgia dos sistemas lacrimal e nasolacrimal do cão**. In: Manual de Oftalmologia Veterinária. São Paulo: Manole, p. 73 – 94, 2003.

GELATT, K. N. **Handbook of Small Animal Ophthalmic Surgery, Extraocular Procedures**. Gainesville, FL: Pergamon Press, p. 125 – 135, 1995.

GRAHN, B. H.; SANDMEYER, L. S. **Diseases and surgery of the canine nasolacrimal system**. In: Gelatt KN, ed. *Veterinary ophthalmology*. Ames, Iowa: Blackwell Publishing, 618–632, 2007.

HABIN, D. **The nasolacrimal system**. In: Petersen-jones, S. M., Crispin, S. M. Manual of Small Animal Ophthalmology. Shurdington: British Small Animal Veterinary Association, 1993.

HOU, K.; AI, T.; LIU, R.; XIANG, N.; JIN, J.; HU, W.; & LUO, B. Modeling Chronic Dacryocystitis in Rabbits by Nasolacrimal Duct Obstruction with Self-Curing Resin. **Journal of Ophthalmology,** v. 1, n. 1, p. 1–8, 2017.

JUGANT, S.; ROBIN, M.; REGNIER, A.; CASSARD, H.; HERMAN, N.; CONCHOU, F. & DOUET, J. Congenital lacrimal fistula in two prim'Holstein calves. **Veterinary Ophthalmology**, p. 1-6, 2019.

KANSKI, J. J. **Distúrbio do sistema de drenagem lacrimal**. In: Ibid. (publishing company), Oftalmologia Clínica: uma abordagem sistemática. 4ª edition. Rio de Janeiro: Revinter, 43-54, 2004a.

KANSKI, J. J. **Sistema de drenagem lacrimal**. In: Ibid. (publishing company), Oftalmologia Clínica: uma abordagem sistemática. 5ª edition. Rio de Janeiro: Elsevier, Rio de Janeiro. 43-55, 2004b.

KERN, T. J. **Disorders of the lacrimal system**. In: Kirk RW, ed. Current veterinary therapy IX. Philadephia: WB Saunders Co, 634–641, 1986.

KUMAR, V. A.; ESMAELI, B.; AHMED, S.; GOGIA, B.; DEBNAM, J. M.; AND GINSBERG, L. E. Imaging Features of Malignant Lacrimal Sac and Nasolacrimal Duct Tumors. **American Journal of Neuroradiology,** v. 37, n. 11, p. 2134-2137, 2016.

KÜNZEL, W.; BREIT, S.; & OPPEL, M. Morphometric investigations of breed-specific features in feline skulls and considerations on their functional implications. **Anatomia Histologia Embryologia**, v. 32, n. 4, p. 218-23, 2003.

MICHEL, G. Beitrag zur Anatomie der Tränenorgane von Hund und Katze. Deutsche. **Tierärztliche Wochenschrft**, v. 62, p. 347–349, 1955.

NJAA, B. L.; COLE, L. K.; & TABACCA, N. Practical Otic Anatomy and Physiology of the Dog and Cat. **Veterinary Clinics of North America: Small Animal Practice**, v. 42, n. 6, p. 1109–1126, 2012.

NOMINA ANATOMICA VETERINARIA (NAV). **International Committee on Veterinary Gross Anatomical Nomenclature**. 6ª ed. Hanover (Germany), Ghent (Belgium), Columbia, MO (U.S.A.), Rio de Janeiro (Brazil), 2017.

NÖLLER, C.; WOLFGANG, H.; DIETRICH, H. W.; GRÖNEMEYER, R. M.; HIRSCHBERG, K. D. B. Computed tomography-anatomy of the normal feline nasolacrimal drainage system. **Veterinary Radiology & Ultrasound**, v. 47, n. 1, p. 53–60, 2006.

NYKAMP, S. G.; SCRIVANI, P. V.; PEASE, A. P. Computed tomography dacryocystography evaluation of the nasolacrimal apparatus. **Veterinary Radiology & Ultrasound**, v. 45, n. 1, p. 23-31, 2004.

OLLIVIER, F. J.; PLUMMER, C. E.; BARRIE, K. P. **Ophthalmic examination and diagnostics. Part 1: the eye examination and diagnostic procedures**. In: Gelatt KN, ed. Veterinary ophthalmology. 4th ed. Ames, Iowa: Blackwell Publishing, 438–483, 2007.

PAIVA, S. C. S.; FROES, T. R.; LANGE, R. R.; MACHADO, M.; PACHALY, J. R.; MONTIANI-FERREIRA F. Iatrogenic Nasolacrimal Duct Obstruction Following Tooth Extraction in a Cat. **Journal of Veterinary Dentistry**, v. 30, n. 2, p. 90–94, 2013.

PARK, S. A.; TAYLOR, K. T.; ZWINGENBERGER, A. L.; REILLY, C. M.; TOUPADAKIS, C. A.; MARFURT, C. F.; GOOD, K. L.; MURPHY, C. J. Gross anatomy and morphometric evaluation of the canine lacrimal and third eyelid glands. **Veterinary Ophthalmology**, v. 19, n. 3, p. 230–236, 2016.

RACHED, P. A.; CANOLA, J. C.; SCHLUTER, C.; LAUS, J. L.; OECTHERING, G.; ALMEIDA, D. E.; LUDWIG E. Computed tomographic-dacryocystography (CT-DCG) of the normal canine nasolacrimal drainage system with three-dimensional reconstruction. **Veterinary Ophthalmology**, v. 14, n. 3, p. 174–179, 2011.

RAMSEY, D. T.; MARRETTA, S. M.; HAMOR, R. E.; GERDING, P. A. JR.; KNIGHT, B.; JOHNSON, J. M; BAGLEY, L. H. Ophthalmic manifestations and complications of dental disease in dogs and cats. **Journal of the American Animal Hospital Association**, v. 32, p. 215–224, 1996.

SAPIENZA, J.; ISAZA, R.; JOHNSON, R.; MILLER, T. Anatomic and radiographic study of the lacrimal apparatus of llamas. **American Journal Veterinary Research**, v. 53, n. 6, p. 1007–1009, 1992.

SPIESS, B. M.; POT, S. A. Diseases and Surgery of the Canine Orbit. In: Gelatt, K. N. (Ed.). **Veterinary Ophthalmology**, 5th edition. Wiley Blackwell, Ames, Iowa, USA, 793–831, 2013.

SCHLUETER, C.; BUDRAS, K. D.; LUDEWIG, E.; MAYRHOFER, E.; KOENIG, H. E.; & WALTER, A. Brachycephalic feline noses: CT and anatomical study of the relationship between head conformation and the nasolacrimal drainage system. **Journal of Feline Medicine and Surgery,** v. 11, n. 11, p. 891–900, 2009.

SHOKRY, M.; ABDEL HAMID, M. A.; AHMED, A. S.; AND IBRAHIM, I. M. Radiography of the nasolacrimal duct in the dromedary (Camelus Dromedarius). **Journal of Zoo Animal Medicine**, v. 18, n. 2, p. 94-95, 1987.

STADES, F. C.; BOEVÉ, M. H.; NEUMANN, W. **Fundamentos de Oftalmologia Veterinária**. São Paulo: Manole, 1999. 204p, 1999.

STILES, J.; TOWNSEND W. M. **Feline Ophthalmology**. In: Veterinary Ophthalmology, 4th edition (Gelatt KN publishing company). Iowa: Blackwell Publishing. 1095–1164, 2007.

TAKAHASHI, Y.; KAKIZAKI, H.; & NAKANO, T. Bony nasolacrimal duct entrance diameter: gender difference in cadaveric study. **Ophthalmology Plastic and Reconstructive Surgery**, v. 27, n. 3, p. 204-205. 2011.

TAKEHARA, Y.; ISODA, H.; KURIHASHI, K.; ISOGAI, S. Dynamic MR dacryocystography: a new method for evaluating nasolacrimal duct obstructions. **American Journal of Roentgenology**, v. 175, n. 2, p. 469–473, 2000.

THALE, A.; PAULSEN, F.; ROCHELS, R.; TILLMANN, B. Functional anatomy of the human efferent tear ducts: a new theory of tear outflow mechanism. **Graefe's Archive for Clinical and Experimental Ophthalmology**, v. 236, n. 9, p. 674, 1998.

VOELTER-RATSON, K.; HAGEN, R.; GRUNDMANN, S.; & SPIESS, B. M. Dacryocystitis following a nasolacrimal duct obstruction caused by an ectopic intranasal tooth in a dog. **Veterinary Ophthalmology**, v. 18, n. 5, p. 433–436, 2014.

WORLEY, G.; STURNER, R. A.; GREEN, J. A.; FROTHINGHAM, T. E. Evidence for a Relationship Between Head Shape and Prevalence of Middle Ear Effusion in Children. **Clinical Anatomy**, v. 7, p. 84-89, 1994.

YONG, A. M.; ZHAO, D. B.; SIEW, S. C.; GOH, P. S.; LIAO, J. & AMRITH, S. Assessment of bony nasolacrimal parameters among Asians. **Ophthalmology Plastic and Reconstructive Surgery**, v. 30, n. 4, p. 322-377, 2014.

YOSHIKAWA, T.; HIROTA, S.; SUGIMURA, K. Topical contrast-enhanced magnetic resonance dacryocystography. **Radiation Medicine**, v. 18, n. 6, p. 355-362. 2000.

CAPÍTULO 4

CONSIDERAÇÕES FINAIS

CONSIDERAÇÕES FINAIS

Com base nas análises e resultados apresentados, além da literatura citada, ao longo do presente manuscrito, pode-se afirmar que a braquicefalia em felinos domésticos pode ser definida objetivamente, com base em índices craniométricos e contribuindo para a classificação dos fenótipos cranianos.

As metodologias utilizadas para identificar crânios felinos braquicefálicos e não braquicefálicos foram eficientes e podem ser facilmente reproduzidas e utilizadas na prática clínico-cirúrgica de felinos domésticos. Vislumbra-se validar a metodologia empregada neste estudo com outras populações de felinos de diferentes raças, utilizando-se da análise de tomografias de centros de diagnósticos por imagens e de testes estatísticos adequados.

O ducto nasolacrimal de gatos da raça Persa possui características morfológicas peculiares, associadas ao formato craniano braquicefálico e relacionadas com a epífora nesses animais.